Eur. Phys. J. C 27, 497–521 (2003)
Digital Object Identifier (DOI) 10.1140/epjc/s2003-01136-2

THE EUROPEAN PHYSICAL JOURNAL C

Confronting spectral functions from e^+e^- annihilation and τ decays: consequences for the muon magnetic moment

M. Davier[1,a], S. Eidelman[2,b], A. Höcker[1,c], Z. Zhang[1,d]

[1] Laboratoire de l'Accélérateur Linéaire, IN2P3-CNRS et Université de Paris-Sud, 91898 Orsay, France
[2] Budker Institute of Nuclear Physics, Novosibirsk, 630090, Russia

Received: 27 August 2002 / Revised version: 10 January 2003 /
Published online: 26 February 2003 –

Abstract. Vacuum polarization integrals involve the vector spectral functions which can be experimentally determined from two sources: (*i*) e^+e^- annihilation cross sections and (*ii*) hadronic τ decays. Recently results with comparable precision have become available from CMD-2 on one side, and ALEPH, CLEO and OPAL on the other. The comparison of the respective spectral functions involves a correction from isospin-breaking effects, which is evaluated. After the correction it is found that the dominant $\pi\pi$ spectral functions do not agree within experimental and theoretical uncertainties. Some disagreement is also found for the 4π spectral functions. The consequences of these discrepancies for vacuum polarization calculations are presented, with the emphasis on the muon anomalous magnetic moment. The work includes a complete re-evaluation of all exclusive cross sections, taking into account the most recent data that became available in particular from the Novosibirsk experiments and applying corrections for the missing radiative corrections. The values found for the lowest-order hadronic vacuum polarization contributions are

$$a_\mu^{\rm had,LO} = \begin{cases} (684.7 \pm 6.0_{\rm exp} \pm 3.6_{\rm rad})\ 10^{-10} & [e^+e^-\text{−based}]\ , \\ (709.0 \pm 5.1_{\rm exp} \pm 1.2_{\rm rad} \pm 2.8_{\rm SU(2)})\ 10^{-10} & [\tau\text{−based}]\ , \end{cases}$$

where the errors have been separated according to their sources: experimental, missing radiative corrections in e^+e^- data, and isospin breaking. The Standard Model predictions for the muon magnetic anomaly read

$$a_\mu = \begin{cases} (11\,659\,169.3 \pm 7.0_{\rm had} \pm 3.5_{\rm LBL} \pm 0.4_{\rm QED+EW})\ 10^{-10} & [e^+e^-\text{−based}]\ , \\ (11\,659\,193.6 \pm 5.9_{\rm had} \pm 3.5_{\rm LBL} \pm 0.4_{\rm QED+EW})\ 10^{-10} & [\tau\text{−based}]\ , \end{cases}$$

where the errors account for the hadronic, light-by-light scattering and electroweak contributions. We observe deviations with the recent BNL measurement at the 3.0 (e^+e^-) and 0.9 (τ) σ level, when adding experimental and theoretical errors in quadrature.

Contents

[a] e-mail: davier@lal.in2p3.fr
[b] e-mail: simon.eidelman@cern.ch
[c] e-mail: hoecker@lal.in2p3.fr
[d] e-mail: zhangzq@lal.in2p3.fr

1 Introduction

Hadronic vacuum polarization in the photon propagator plays an important role in the precision tests of the Standard Model. This is the case for the evaluation of the electromagnetic coupling at the Z mass scale, $\alpha(M_Z^2)$, which receives a contribution $\Delta\alpha_{\rm had}(M_Z^2)$ of the order of 2.8 10^{-2} that must be known to an accuracy of better than 1% so that it does not limit the accuracy on the indirect determination of the Higgs boson mass from the measurement of $\sin^2\theta_W$. Another example is provided by the anomalous magnetic moment $a_\mu = (g_\mu - 2)/2$ of the muon where the hadronic vacuum polarization component is the leading contributor to the uncertainty of the theoretical prediction.

Starting from [1,2] there is a long history of calculating the contributions from hadronic vacuum polarization in these processes. As they cannot be obtained from first principles because of the low energy scale involved, the computation relies on analyticity and unitarity so that the relevant integrals can be expressed in terms of an experimentally determined spectral function which is proportional to the cross section for e^+e^- annihilation into hadrons. The accuracy of the calculations has therefore followed the progress in the quality of the corresponding data [3]. Because the latter was not always suitable, it was deemed necessary to resort to other sources of information. One such possibility was the use [4] of the vector spectral functions derived from the study of hadronic τ decays [5] for the energy range less than 1.8 GeV. Another one occurred when it was realized in the study of τ decays [6] that perturbative QCD could be applied to energy scales as low as 1-2 GeV, thus offering a way to replace poor e^+e^- data in some energy regions by a reliable and precise theoretical prescription [7–9]. Finally, without any further theoretical assumption, it was proposed to use QCD sum rules [10,11] in order to improve the evaluation in energy regions dominated by resonances where one has to rely on experimental data. Using these improvements the lowest-order hadronic contribution to a_μ was found to be [11]

$$a_\mu^{\rm had,LO} \;=\; (692.4 \pm 6.2)\; 10^{-10}\;. \qquad (1)$$

The complete theoretical prediction includes in addition QED, weak and higher order hadronic contributions.

The anomalous magnetic moment of the muon is experimentally known to very high accuracy. Combined with the older, less precise results from CERN [12], the measurements from the E821 experiment at BNL [13–15], including the most recent result [16], yield

$$a_\mu^{\rm exp} \;=\; (11\,659\,203 \pm 8)\; 10^{-10}\;, \qquad (2)$$

and are aiming at an ultimate precision of 4 10^{-10} in the future. The previous experimental result [15] was found to deviate from the theoretical prediction by 2.6 σ, but a large part of the discrepancy was actually originating from a sign mistake in the calculation of the small contribution from the so-called light-by-light (LBL) scattering diagrams [17,18]. The new calculations of the LBL contribution [19–21] have reduced the discrepancy to a nonsignificant 1.6 σ level. At any rate it is clear that the presently achieved experimental accuracy already calls for a more precise evaluation of $a_\mu^{\rm had,LO}$.

In this paper we critically review the available experimental input to vacuum polarization integrals. Such a re-evaluation is necessary because

- new results have been obtained at Novosibirsk with the CMD-2 detector in the region dominated by the ρ resonance [22] with a much higher precision than before, and more accurate R measurements have been performed in Beijing with the BES detector in the 2-5 GeV energy range [23].
- new preliminary results are available from the final analysis of τ decays with ALEPH using the full statistics accumulated at LEP1 [24]; also the information from the spectral functions measured by CLEO [25, 26] and OPAL [27] was not used previously and can be incorporated in the analysis.
- new results on the evaluation of isospin breaking have been produced [28–30], thus providing a better understanding of this critical area when relating vector τ and isovector e^+e^- spectral functions.

Since we are mostly dealing with the low energy region, common to both e^+e^- and τ data, and because of the current interest in the muon magnetic moment prompted by the new experimental result, the emphasis in this paper is on $a_\mu^{\rm had,LO}$ rather than $\Delta\alpha_{\rm had}(M_Z^2)$. It is true that the presently achieved accuracy on $\Delta\alpha_{\rm had}(M_Z^2)$ is meeting the goals for the LEP/SLD/FNAL global electroweak fit. However the situation will change in the long run when very precise determinations of $\sin^2\theta_{\rm W}$, as could be available from the beam polarization asymmetry at the future Linear Collider, necessitate a significant increase of the accuracy on $\Delta\alpha_{\rm had}(M_Z^2)$[31].

Disclaimer: 'theoretical' predictions using vacuum polarization integrals are based on experimental data as input. The data incorporated in this analysis are used as quoted by their authors. In particular, no attempt has been made to re-evaluate systematic uncertainties even if their size was deemed to be questionable in some cases. However, whenever significant incompatibilities between experiments occur, we apply an appropriate rescaling of the combined error. The analysis thus heavily relies on the quality of the work performed in the experiments.

2 Muon magnetic anomaly

It is convenient to separate the Standard Model prediction for the anomalous magnetic moment of the muon into its different contributions,

$$a_\mu^{\rm SM} \;=\; a_\mu^{\rm QED} + a_\mu^{\rm had} + a_\mu^{\rm weak} \;, \qquad (3)$$

with

$$a_\mu^{\rm had} \;=\; a_\mu^{\rm had,LO} + a_\mu^{\rm had,HO} + a_\mu^{\rm had,LBL} \;, \qquad (4)$$

where $a_\mu^{\rm QED} = (11\,658\,470.6 \pm 0.3)\ 10^{-10}$ is the pure electromagnetic contribution (see [32,33] and references therein), $a_\mu^{\rm had,LO}$ is the lowest-order contribution from hadronic vacuum polarization, $a_\mu^{\rm had,HO} = (-10.0 \pm 0.6)\ 10^{-10}$ is the corresponding higher-order part [34,4], and $a_\mu^{\rm weak} = (15.4 \pm 0.1 \pm 0.2)\ 10^{-10}$, where the first error is the hadronic uncertainty and the second is due to the Higgs mass range, accounts for corrections due to exchange of the weakly interacting bosons up to two loops [35]. For the LBL part we add the values for the pion-pole contribution [19–21] and the other terms [20,21] to obtain $a_\mu^{\rm had,LBL} = (8.6 \pm 3.5)\ 10^{-10}$.

By virtue of the analyticity of the vacuum polarization correlator, the contribution of the hadronic vacuum polarization to a_μ can be calculated via the dispersion integral [36]

$$a_\mu^{\rm had,LO} \;=\; \frac{\alpha^2(0)}{3\pi^2} \int\limits_{4m_\pi^2}^{\infty} ds\, \frac{K(s)}{s} R(s) \;, \qquad (5)$$

where $K(s)$ is the QED kernel [37] ,

$$K(s) = x^2 \left(1 - \frac{x^2}{2}\right) + (1+x)^2 \left(1 + \frac{1}{x^2}\right) \times \left(\ln(1+x) - x + \frac{x^2}{2}\right) + \frac{(1+x)}{(1-x)} x^2 \ln x \;, \qquad (6)$$

with $x = (1-\beta_\mu)/(1+\beta_\mu)$ and $\beta_\mu = (1 - 4m_\mu^2/s)^{1/2}$. In (5), $R(s) \equiv R^{(0)}(s)$ denotes the ratio of the 'bare' cross section for e^+e^- annihilation into hadrons to the pointlike muon-pair cross section. The 'bare' cross section is defined as the measured cross section, corrected for initial state radiation, electron-vertex loop contributions and vacuum polarization effects in the photon propagator (see Sect. 4 for details). The reason for using the 'bare' (i.e. lowest order) cross section is that a full treatment of higher orders is anyhow needed at the level of a_μ, so that the use of 'dressed' cross sections would entail the risk of double-counting some of the higher-order contributions.

The function $K(s)$ decreases monotonically with increasing s. It gives a strong weight to the low energy part of the integral (5). About 91% of the total contribution to $a_\mu^{\rm had,LO}$ is accumulated at center-of-mass energies $\sqrt{s}$ below 1.8 GeV and 73% of $a_\mu^{\rm had,LO}$ is covered by the two-pion final state which is dominated by the $\rho(770)$ resonance.

3 The input data

3.1 e^+e^- annihilation data

The exclusive low energy e^+e^- cross sections have been measured mainly by experiments running at e^+e^- colliders in Novosibirsk and Orsay. Due to the high hadron multiplicity at energies above $\sim$ 2.5 GeV, the exclusive measurement of the respective hadronic final states is not practicable. Consequently, the experiments at the high energy colliders ADONE, SPEAR, DORIS, PETRA, PEP, VEPP-4, CESR and BEPC have measured the total inclusive cross section ratio R.

We give in the following a compilation of the data used in this analysis:

- The $e^+e^- \to \pi^+\pi^-$ measurements are taken from OLYA [38,39], TOF [40], CMD [38], DM1 [41] and DM2 [42].
  The most precise data from CMD-2 are now available in their final form [22]. They differ from the preliminary ones, released two years ago [43], mostly in the treatment of radiative corrections. Compared to the preliminary ones, the new results are corrected (see Sect. 4) for leptonic and hadronic vacuum polarization, and for photon radiation by the pions (final state radiation – FSR), so that the measured final state corresponds to $\pi^+\pi^-$ including pion-radiated photons. The various changes resulted in a reduction of the cross section by about 1% below the ρ peak and 5% above. The dominant contribution stemmed from vacuum polarization, while the (included) FSR correction increased the cross section by about 0.8% in the peak region. The overall systematic error of the final data is quoted to be 0.6% and is dominated by the uncertainties in the radiative corrections (0.4%).
  We do not use the data from NA7 [44] as they are known to suffer from a systematic bias in the energy scale [45]. All the experiments agree with each other within their quoted errors, but the high precision claimed by CMD-2 makes this experiment unique and consequently not cross-checked by the others at that level.
  The comparison between the cross section results from CMD-2 and from previous experiments (corrected for vacuum polarization and FSR, according to the procedure discussed in Sect. 4) is shown in Fig. 1. Note that the errors bars given contain both statistical and systematic errors, added in quadrature (this is the case for all figures in this paper). The agreement is good within the much larger uncertainties (2-10%) quoted by the older experiments.
- The situation of the data on the ω and ϕ resonances has significantly improved recently [46–48]. The numerical procedure for integrating their cross sections is described in detail in Sect. 8.2.
- The cross sections for $e^+e^- \to \pi^0\gamma$ and $\eta\gamma$ not originating from the decay of the ω and ϕ resonances are taken from SND [49] and CMD-2 [50] data in the continuum. They include contributions from $\rho \to \pi^0\gamma$ and $\rho \to \eta\gamma$.
- The reaction $e^+e^- \to \pi^+\pi^-\pi^0$ is dominated by the ω and ϕ intermediate resonances discussed above. The continuum data are taken from ND [51], DM1 [52], DM2 [53], SND [54] and CMD [55].
- The $e^+e^- \to \pi^+\pi^-\pi^0\pi^0$ data are available from M3N [56], OLYA [57], ND [51], DM2 [58–60], CMD-2 [61]

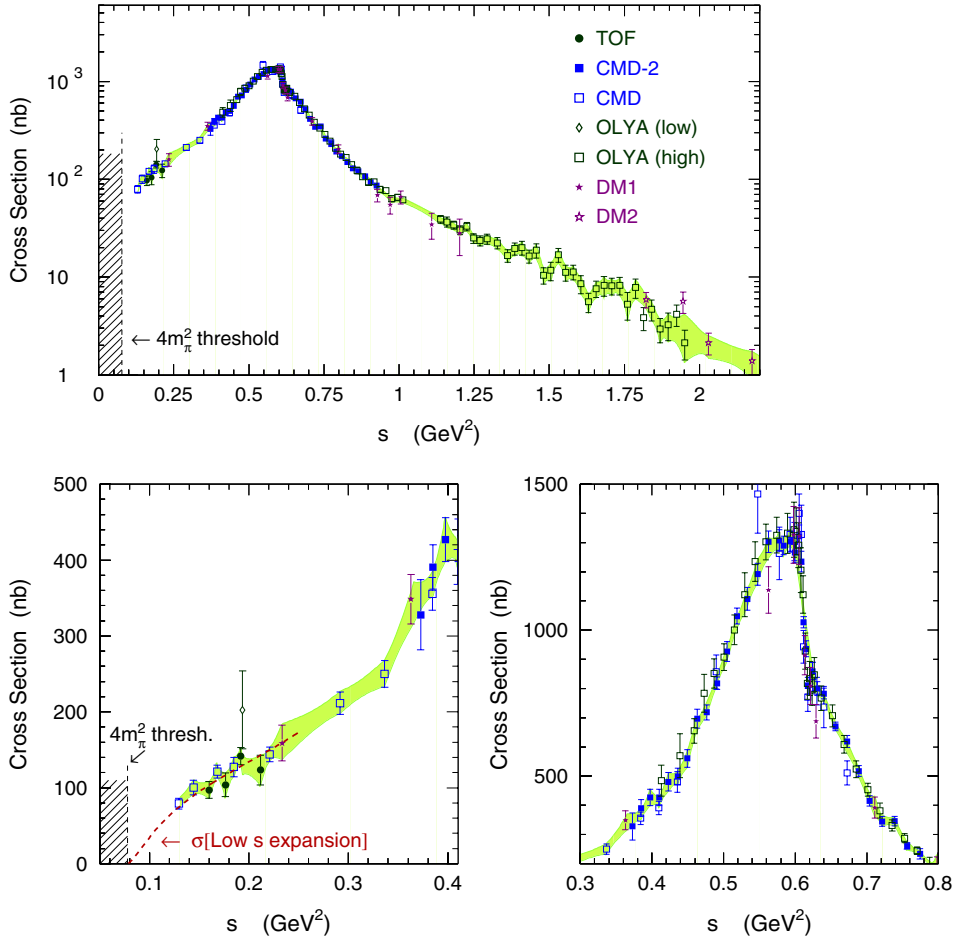

Fig. 1. The cross section for $e^+e^- \to \pi^+\pi^-(\gamma)$ measured by the different experiments. The errors bars contain both statistical and systematic errors, added in quadrature. The band is the combination of all the measurements used for the numerical integration following the procedure discussed in Sect. 7

and SND [62]. It is fair to say that large discrepancies are observed between the different results, which are probably related to problems in the calculation of the detection efficiency (the cross sections can be seen in Fig. 9 shown in Sect. 6.1). The efficiencies are small in general ($\sim 10-30\%$) and are affected by uncertainties in the decay dynamics that is assumed in the Monte Carlo simulation. One could expect the more recent experiments (CMD-2 and SND) to be more reliable in this context because of specific studies performed in order to identify the major decay processes involved. Accordingly we do not include the ND data in the analysis.

– The reaction $e^+e^- \to \omega\pi^0$ is mainly reconstructed in the $\pi^+\pi^-\pi^0\pi^0$ final state and is thus already accounted for. It was studied by the collaborations ND [51], DM2 [59], CMD-2 [61] and SND [62,63]. We use these cross section measurements to compute the contribution corresponding to the $\omega \to \pi^0\gamma$ decay mode.

– The $e^+e^- \to \pi^+\pi^-\pi^+\pi^-$ final state was studied by the experiments OLYA [64], ND [51], CMD [65], DM1 [66, 67], DM2 [58–60], CMD-2 [61] and SND [62]. The experiments agree reasonably well within their quoted uncertainties (see Fig. 8 in Sect. 6.1).

– The $e^+e^- \to \pi^+\pi^-\pi^+\pi^-\pi^0$ data are taken from M3N [56] and CMD [65]. It contains a contribution from the $\eta\pi^+\pi^-$ channel with $\eta \to \pi^+\pi^-\pi^0$ which has to be treated separately because the η decay violates isospin. The other five-pion mode $e^+e^- \to \pi^+\pi^-3\pi^0$ is not measured, but can be accounted for using the isospin relation $\sigma_{\pi^+\pi^-3\pi^0} = \sigma_{\pi^+\pi^-\pi^+\pi^-\pi^0}/2$. The relation is used after subtracting the $\eta\pi^+\pi^-$ contribution in the $\pi^+\pi^-\pi^+\pi^-\pi^0$ rate. Then the $\eta\pi^+\pi^-$ contribution with $\eta \to 3\pi^0$ is added to obtain the full $\pi^+\pi^-3\pi^0$ rate.

– For the reaction $e^+e^- \to \omega\pi^+\pi^-$, measured by the groups DM1 [68], DM2 [53] and CMD-2 [69], a contribution is calculated for ω decaying into $\pi^0\gamma$. The dominant three-pion decay already appears in the five-pion final state.

– Similarly, the contribution for $e^+e^- \to \omega 2\pi^0$, with $\omega \to \pi^0\gamma$, is taken by isospin symmetry to be half of $e^+e^- \to \omega\pi^+\pi^-$.

– The process $e^+e^- \to \eta\pi^+\pi^-$ was studied by ND [51], DM2 [53] and CMD-2 [69]. We subtract from its cross section the contributions which are already counted in the $\pi^+\pi^-\pi^+\pi^-\pi^0$ and $\pi^+\pi^-3\pi^0$ final states.

– The cross sections of the six-pion final states $3\pi^+3\pi^-$ and $2\pi^+2\pi^-2\pi^0$ were measured by DM1 [70], CMD [65] and DM2 [71]. For the missing channel $\pi^+\pi^-4\pi^0$ one can rely on isospin relations in order to estimate its contribution. If only e^+e^- data are used, the isospin

bound [4] is weak, leading to a possibly large contribution with an equally large uncertainty. However, some information can be found in the isospin-rotated processes[1] $\tau^- \to \nu_\tau\, 3\pi^- 2\pi^+\pi^0$ and $\tau^- \to \nu_\tau\, 2\pi^-\pi^+ 3\pi^0$, where the hadronic system has been shown [72] to be dominated by $\omega 2\pi^-\pi^+$ and $\omega\pi^- 2\pi^0$, once the axial-vector $\eta 2\pi^-\pi^+$ and $\eta\pi^- 2\pi^0$ contributions [73] are discarded. An isospin analysis then reveals the dominance of the $\omega\rho^\pm\pi^\mp$ final state. As a consequence the $\pi^+\pi^- 4\pi^0$ channel in e^+e^- annihilation only receives a very small contribution, determined by the $3\pi^+3\pi^-$ cross section. We include a component for $\omega \to \pi^0\gamma$.

- The $e^+e^- \to K^+K^-$ and $e^+e^- \to K^0_S K^0_L$ cross sections above the ϕ resonance are taken from OLYA [74], DM1 [75], DM2 [76], CMD [77] and CMD-2 [78].
- The reactions $e^+e^- \to K^0_S K^\pm\pi^\mp$ and $e^+e^- \to K^+K^-\pi^0$ were studied by DM1 [79,80] and DM2 [58]. Using isospin symmetry the cross section of the final state $K^0_S K^0_L\pi^0$ is obtained from the relation $\sigma_{K^0_S K^0_L\pi^0} = \sigma_{K^+K^-\pi^0}$.
- The inclusive reaction $e^+e^- \to K^0_S + X$ was analyzed by DM1 [81]. After subtracting from its cross section the separately measured contributions of the final states $K^0_S K^0_L$, $K^0_S K^\pm\pi^\mp$ and $K^0_S K^0_L\pi^0$, it still includes the modes $K^0_S K^0_S\pi^+\pi^-$, $K^0_S K^0_L\pi^+\pi^-$ and $K^0_S K^\pm\pi^\mp\pi^0$. With the assumption that the cross sections for the processes $e^+e^- \to K^0\overline{K}^0(\pi\pi)^0$ and $e^+e^- \to K^+K^-(\pi\pi)^0$ are equal, one can summarize the total $K\overline{K}\pi\pi$ contribution as twice the above corrected $K^0_S + X$ cross section. Implied by the assumption made, it is reasonable to quote as the systematic uncertainty one-half of the cross section for the channel $K^+K^-\pi^+\pi^-$ measured by DM1 [79] and DM2 [82].
- Baryon-pair production is included using the cross sections for $p\overline{p}$ from DM1 [83] and DM2 [84], and for $n\overline{n}$ from FENICE [85].
- At energies larger than 2 GeV the total cross section ratio R is measured inclusively. Data are provided by the experiments $\gamma\gamma 2$ [86], MARK I [87], DELCO [88], DASP [89], PLUTO [90], LENA [91], Crystal Ball [92,93], MD-1 [94], CELLO [95], JADE [96], MARK-J [97], TASSO [98], CLEO [99], CUSB [100], MAC [101], and BES [23]. Due to their weak experimental precision, the data of $\gamma\gamma 2$ are not used in this analysis. The measurements of the MARK I Collaboration are significantly higher than those from more recent and more precise experiments. In addition, the QCD prediction of R, which should be reliable in this energy regime, favours lower values, in agreement with the other experiments. Consequently the MARK I results on R have been discarded.
  Although small, the enhancement of the cross section due to $\gamma - Z$ interference is corrected for energies above the J/ψ mass. We use a factorial ansatz according to [102,3], yielding a negligible contribution to $a_\mu^{\rm had,LO}$.

[1] Throughout this paper, charge conjugate states are implied for τ decays

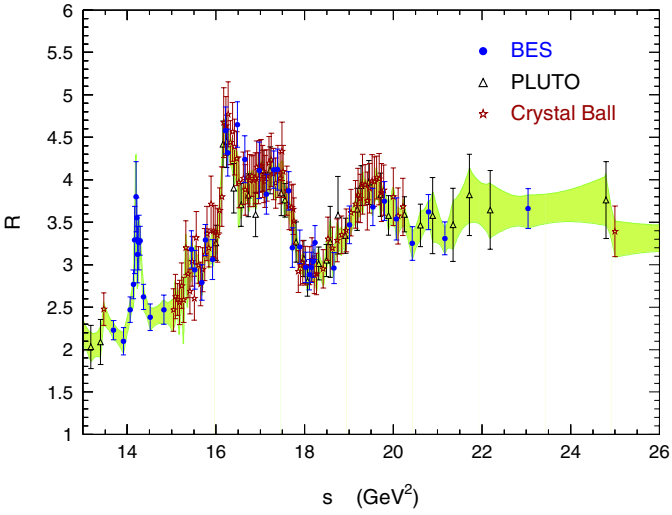

Fig. 2. R data in the charm region. The band is the combination of all the measurements used for the numerical integration following the procedure discussed in Sect. 7

The R data in the charm region are displayed in Fig. 2. Good agreement is found among the experiments.

- The narrow $c\bar{c}$ and $b\bar{b}$ resonances are treated in Sect. 8.3.

3.2 Data from hadronic τ decays

Data from τ decays into two- and four-pion final states $\tau^- \to \nu_\tau\pi^-\pi^0$, $\tau^- \to \nu_\tau\pi^- 3\pi^0$ and $\tau^- \to \nu_\tau 2\pi^-\pi^+\pi^0$, are available from ALEPH [5], CLEO [25,26] and OPAL [27]. Very recently, preliminary results on the full LEP1 statistics have been presented by ALEPH [24]. They agree with the published results, but correspond to a complete reanalysis with refined systematic studies allowed by the 2.5 times larger data set. The branching fraction $B_{\pi\pi^0}$ for the $\tau \to \nu_\tau\,\pi^-\pi^0\ (\gamma)$ decay mode is of particular interest since it provides the normalization of the corresponding spectral function. The new value [24], $B_{\pi\pi^0} = (25.47 \pm 0.13)\%$, turns out to be larger than the previously published one [103] based on the 1991-93 LEP1 statistics, $(25.30 \pm 0.20)\%$.

Assuming (for the moment) isospin invariance to hold, the corresponding e^+e^- isovector cross sections are calculated via the CVC relations

$$\sigma^{I=1}_{e^+e^-\to\pi^+\pi^-} = \frac{4\pi\alpha^2}{s}\, v_{\pi^-\pi^0}\ , \tag{7}$$

$$\sigma^{I=1}_{e^+e^-\to\pi^+\pi^-\pi^+\pi^-} = 2\cdot\frac{4\pi\alpha^2}{s}\, v_{\pi^- 3\pi^0}\ , \tag{8}$$

$$\sigma^{I=1}_{e^+e^-\to\pi^+\pi^-\pi^0\pi^0} = \frac{4\pi\alpha^2}{s}\,\left[v_{2\pi^-\pi^+\pi^0} - v_{\pi^- 3\pi^0}\right]\ . \tag{9}$$

The τ spectral function $v_V(s)$ for a given vector hadronic state V is defined by [104]

$$v_V(s) \equiv \frac{m_\tau^2}{6\,|V_{ud}|^2\, S_{\rm EW}}\,\frac{B(\tau^- \to \nu_\tau\, V^-)}{B(\tau^- \to \nu_\tau\, e^-\,\bar{\nu}_e)}\,\frac{dN_V}{N_V\, ds}$$

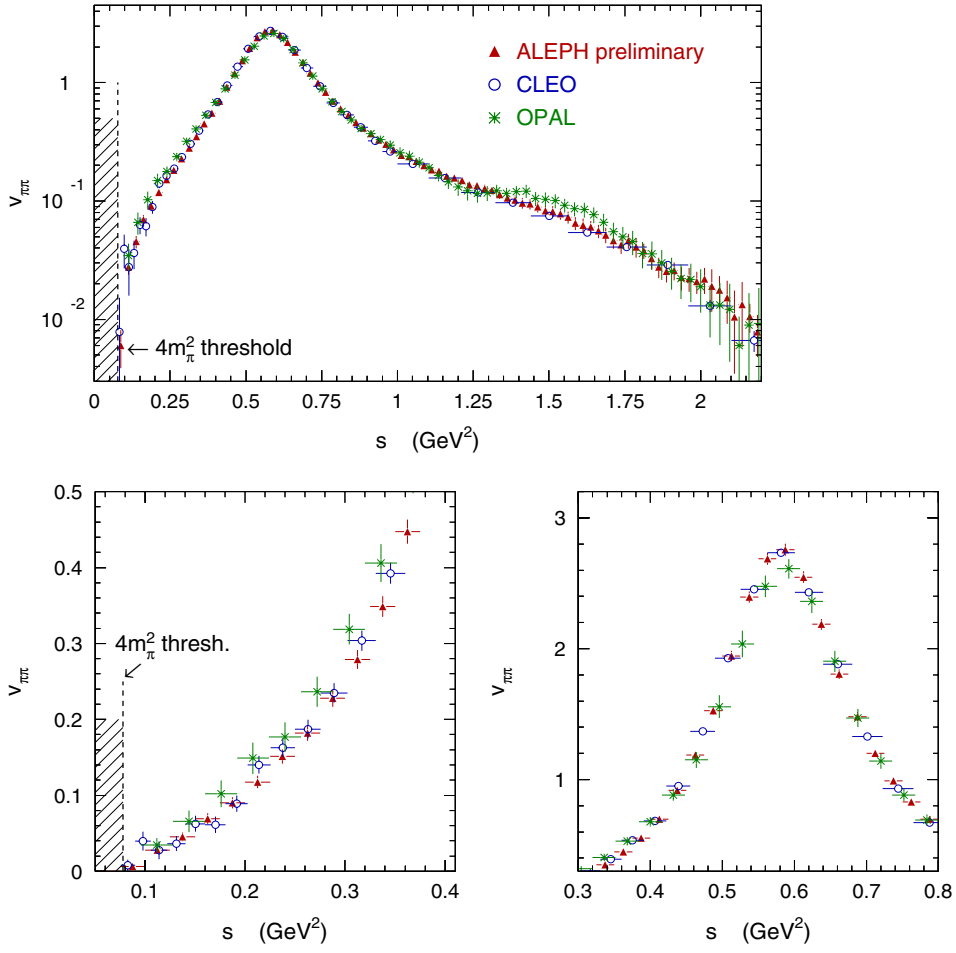

Fig. 3. Comparison between the shapes of the ALEPH, CLEO and OPAL $\pi\pi$ spectral functions normalized to the world-average branching ratio $B_{\pi\pi^0}$. The normalization errors, correlated between the shapes, are not contained in the error bars

$$\times \left[\left(1-\frac{s}{m_\tau^2}\right)^2\left(1+\frac{2s}{m_\tau^2}\right)\right]^{-1}, \qquad (10)$$

where $|V_{ud}| = 0.9748 \pm 0.0010$ is obtained from averaging[2] the two independent determinations [105] from nuclear β decays and kaon decays (assuming unitarity of the CKM matrix) and $S_{\rm EW}$ accounts for electroweak radiative corrections as discussed in Sect. 5.1. The spectral functions are obtained from the corresponding invariant mass distributions, after subtracting out the non-τ background and the feedthrough from other τ decay channels, and after a final unfolding from detector effects such as energy and angular resolutions, acceptance, calibration and photon identification.

It is important to note that τ decay experiments measure decay rates that include the possibility of photon radiation in the decay final state. Depending on the experiment, the analysis may (ALEPH) or may not (CLEO) keep events with radiative photons in the final state, but all experiments rely on the TAUOLA τ decay library [106] to compute their efficiencies. In TAUOLA charged particles are given a probability to produce bremsstrahlung using the PHOTOS procedure [107] which is based on the leading logarithm approximation valid at low photon energy. Thus the measured spectral functions correspond to given final states inclusive with respect to radiative photons in the τ decay.

It should be pointed out that the experimental conditions at Z (ALEPH, OPAL) and $\Upsilon(4S)$ (CLEO) energies are very different. On the one hand, at LEP, the $\tau^+\tau^-$ events can be selected with high efficiency ($> 90\%$) and small non-τ background ($< 1\%$), thus ensuring little bias in the efficiency determination. The situation is not as favorable at lower energy: because the dominant hadronic cross section has a smaller particle multiplicity, it is more likely to pollute the τ sample and strong cuts must be applied, hence resulting in smaller efficiencies. On the other hand, CLEO has an advantage for the reconstruction of the decay final state since particles are more separated in space. The LEP detectors have to cope with collimated τ decay products and the granularity of the detectors, particularly the calorimeters, plays a crucial role. One can therefore consider ALEPH/OPAL and CLEO data to be approximately uncorrelated as far as experimental procedures are concerned. The fact that their respective spectral functions for the $\pi^-\pi^0$ and $2\pi^-\pi^+\pi^0$ modes agree, as demonstrated in Fig. 3 for $\pi^-\pi^0$, is therefore a valuable experimental consistency test.

[2] Since the two determinations, $|V_{ud}|_{\rm nucleons} = 0.9734 \pm 0.0008$ and $|V_{ud}|_{\rm kaons} = 0.9756 \pm 0.0006$ are not consistent, the final error has been enlarged correspondingly

4 Radiative corrections for e^+e^- data

Radiative corrections applied to the measured e^+e^- cross sections are an important step in the experimental analyses. They involve the consideration of several physical processes and lead to large corrections. We stress again that the evaluation of the integral in (5) requires the use of the 'bare' hadronic cross section, so that the input data must be analyzed with care in this respect.

Several steps are to be considered in the radiative correction procedure:

- Corrections are applied to the luminosity determination, based on large-angle Bhabha scattering and muon-pair production in the low-energy experiments, and small-angle Bhabha scattering at high energies. These processes are usually corrected for external radiation, vertex corrections and vacuum polarization from lepton loops.
- The hadronic cross sections given by the experiments are always corrected for initial state radiation and the effect of loops at the electron vertex.
- The vacuum polarization correction in the photon propagator is a more delicate point. The cross sections need to be fully corrected for our use, i.e.

$$\sigma_{\rm bare} \;=\; \sigma_{\rm dressed} \left(\frac{\alpha(0)}{\alpha(s)}\right)^2 \;, \qquad (11)$$

where $\sigma_{\rm dressed}$ is the measured cross section already corrected for initial state radiation, and $\alpha(s)$ is obtained from resummation of the lowest-order evaluation

$$\alpha(s) \;=\; \frac{\alpha(0)}{1-\Delta\alpha_{\rm lep}(s)-\Delta\alpha_{\rm had}(s)}. \qquad (12)$$

Whereas $\Delta\alpha_{\rm lep}(s)$ can be analytically calculated (here given to leading order)

$$\Delta\alpha_{\rm lep}(s) \;=\; \frac{\alpha(0)}{3\pi}\sum_l \left(\log\frac{s}{m_l^2}-\frac{5}{3}\right) \;, \qquad (13)$$

$\Delta\alpha_{\rm had}(s)$ is related by analyticity and unitarity to a dispersion integral, akin to (5),

$$\Delta\alpha_{\rm had}(s) \;=\; -\frac{\alpha(0)s}{3\pi}\,{\rm Re}\int\limits_{4m_\pi^2}^{\infty} ds' \,\frac{R(s')}{s'(s'-s-i\epsilon)} \;, \qquad (14)$$

which must also be evaluated using input data. Since the hadronic correction involves the knowledge of $R(s)$ at all energies, including those where the measurements are made, the procedure has to be iterative, and requires experimental as well as theoretical information over a large energy range.

This may explain why the vacuum polarization correction is in general not applied by the experiments to their published cross sections. Here the main difficulty is even to find out whether the correction (and which one? leptonic at least? hadronic?) has actually been used, as unfortunately this is almost never clearly stated in the publications. The new data from CMD-2 [22] are explicitly corrected for both leptonic and hadronic vacuum polarization effects, whereas the preliminary data from the same experiment [43] were not. In fact, what really matters is the correction to the ratio of the hadronic cross section to the cross section for the process used for the luminosity determination. In the simplest case (for example, DM2 for the $\pi^+\pi^-$ channel) of the normalization to the $e^+e^- \to \mu^+\mu^-$ process, the vacuum polarization effects cancel. However, generally the normalization is done with respect to large angle Bhabha scattering events or to both Bhabha and $\mu^+\mu^-$. In the latter case, Bhabha events dominate due to the t-channel contribution. In the $\pi^+\pi^-$ mode, all experiments before the latest CMD-2 results corrected their measured processes ($\pi^+\pi^-$, $\mu^+\mu^-$ and e^+e^-) for radiative effects using $O(\alpha^3)$ calculations which took only leptonic vacuum polarization into account [108,109]. For the other channels, it is harder to find out as information about the luminosity determination and the detailed procedure for radiative corrections is in general not given in the publications. For all e^+e^- experimental results, but the newest $\pi^+\pi^-$ from CMD-2 and DM2, we apply a correction $C_{\rm HVP}$ for the missing hadronic vacuum polarization given by [110]

$$C_{\rm HVP} \;=\; \frac{1-2\Delta\alpha_{\rm had}(s)}{1-2\Delta\alpha_{\rm had}(\bar{t})} \;, \qquad (15)$$

where the correction in the denominator applies to the Bhabha cross section evaluated at a mean value of the squared momentum transfer t, which depends on the angular acceptance in each experiment. A 50% uncertainty is assigned to $C_{\rm HVP}$. For the ω and ϕ resonance cross sections, we were informed that the recent CMD-2 and SND results were not corrected for leptonic vacuum polarization, so in their case we applied a full correction taking into account both leptonic and hadronic components.

- In (5) one must incorporate in $R(s)$ the contributions of all hadronic states produced at the energy $\sqrt{s}$. In particular, radiative effects in the hadronic final state must be considered, i.e., final states such as $V+\gamma$ have to be included.

Investigating the existing data in this respect is also a difficult task. In the $\pi^+\pi^-$ data from CMD-2 [22] most additional photons are experimentally rejected to reduce backgrounds from other channels and the fraction kept is subtracted using the Monte Carlo simulation which includes a model for FSR. Then the full FSR contribution is added back as a correction, using an analytical expression computed in scalar QED (point-like pions) [111]. As this effect was not included in earlier analyses, we applied the same correction to older $\pi^+\pi^-$ data.

In principle one must worry about FSR effects in other channels as well. For the inclusive R measurements it is included by definition. When R is evaluated from

QCD at high energy, the prediction must be corrected for FSR from the quarks, but this is a negligible effect for $a_\mu^{\rm had,LO}$. The situation for the exclusive channels is less clear because it depends on the experimental cuts and whether or not FSR is included in the simulation. Taking as an educated guess the effect in the $\pi^+\pi^-$ channel, we correspondingly correct the contributions to $a_\mu^{\rm had,LO}$ from all remaining exclusive channels by the factor $C_{\rm FSR} = (1.004 \pm 0.004)^{n_c}$ where n_c is the charged particle multiplicity in the final state.

In summary, we correct each e^+e^- experimental result, but those from CMD-2 ($\pi\pi$), by the factor $C_{\rm rad} = C_{\rm HVP}C_{\rm FSR}$. As an illustration of the orders of magnitude involved, the different corrections in the $\pi^+\pi^-$ contribution amount to -2.3% for the leptonic vacuum polarization, $+0.9\%$ for the hadronic vacuum polarization, and $+0.9\%$ for the FSR correction. The correction to the $\pi\pi/ee$ ratio from the missing hadronic vacuum polarization is small, typically 0.56%. Both the vacuum polarization and FSR corrections apply only to experiments other than CMD-2, therefore the overall correction to the $\pi\pi$ channel is considerably reduced.

The uncertainties on the missing vacuum polarization (50%) and the FSR corrections (100%) are conservatively considered to be fully correlated between all channels to which the correction applies. The total error from these missing radiative corrections, taken as the quadratic sum of the two contributions, is given separately for the final results.

5 Isospin breaking in e^+e^- and τ spectral functions

5.1 Sources of isospin symmetry breaking

The relationships (7), (8) and (9) between e^+e^- and τ spectral functions only hold in the limit of exact isospin invariance. This is the Conserved Vector Current (CVC) property of weak decays. It follows from the factorization of strong interaction physics as produced through the γ and W propagators out of the QCD vacuum. However, we know that we must expect symmetry breaking at some level from electromagnetic effects and even in QCD because of the up and down quark mass splitting. Since the normalization of the τ spectral functions is experimentally known at the 0.5% level, it is clear that isospin-breaking effects must be carefully examined if one wants this precision to be maintained in the vacuum polarization integrals. Various identified sources of isospin breaking are considered in this section and discussed in turn.

Because of the dominance of the $\pi\pi$ contribution in the energy range of interest for τ data, we discuss mainly this channel, following our earlier analysis [4]. The corrections on $a_\mu^{\rm had,LO}$ from isospin breaking are given in Table 1. A more complete evaluation is given in the next section. Finally, the 4-pion modes will be briefly discussed.

– Electroweak radiative corrections must be taken into account. Their dominant contribution comes from the short distance correction to the effective four-fermion coupling $\tau^- \to \nu_\tau(d\bar{u})^-$ enhancing the τ amplitude by the factor $(1 + 3\alpha(m_\tau)/4\pi)(1 + 2\overline{Q})\ln(M_Z/m_\tau)$, where $\overline{Q}$ is the average charge of the final state partons [112]. While this correction vanishes for leptonic decays, it contributes for quarks. All higher-order logarithms can be resummed using the renormalization group [112,113], and the short distance correction can be absorbed into an overall multiplicative electroweak correction $S_{\rm EW}^{\rm had}$,

$$S_{\rm EW}^{\rm had} = \left(\frac{\alpha(m_b)}{\alpha(m_\tau)}\right)^{9/19} \left(\frac{\alpha(M_W)}{\alpha(m_b)}\right)^{9/20} \times \left(\frac{\alpha(M_Z)}{\alpha(M_W)}\right)^{36/17}, \quad (16)$$

which is equal to 1.0194 when using the current fermion and boson masses and for consistency [114] the quark-level $\overline{\rm MS}$ expressions for $\alpha(s)$ as given in [115]. The difference between the resummed value and the lowest-order estimate (1.0188) can be taken as a conservative estimate of the uncertainty. QCD corrections to $S_{\rm EW}^{\rm had}$ have been calculated [112,116] and found to be small, reducing its value to 1.0189.
Subleading non-logarithmic short distance corrections have been calculated to order $O(\alpha)$ at the quark level [117], $S_{\rm EW}^{\rm sub,had} = 1+\alpha(m_\tau)(85/12-\pi^2)/(2\pi) \simeq 0.9967$, and for the leptonic width [112], $S_{\rm EW}^{\rm sub,lep} = 1 + \alpha(m_\tau)(25/4 - \pi^2)/(2\pi) \simeq 0.9957$. Summing up all the short distance corrections, one obtains the value for $S_{\rm EW}$ that must be used for the inclusive hadronic width

$$S_{\rm EW}^{\rm inclusive} = \frac{S_{\rm EW}^{\rm had}\, S_{\rm EW}^{\rm sub,had}}{S_{\rm EW}^{\rm sub,lep}} = 1.0199 \pm 0.0006\ . \quad (17)$$

Other uncertainties on the b quark mass, the running of $\alpha(s)$, and QCD corrections are at the 10^{-4} level.
Long distance corrections are expected to be final-state dependent in general. They have been computed for the $\tau^- \to \nu_\tau\pi^-$ decay leading to a total radiative correction of 2.03%[118], which is dominated by the leading logarithm from the short distance contribution. Although very encouraging, this result may not apply to all hadronic τ decays, in particular for the important $\nu_\tau\pi^-\pi^0$ mode. Therefore an uncertainty of 0.0040 was previously assigned to $S_{\rm EW}$ (see the following Sect. 5.2 for more) to cover the final-state dependence of the correction with respect to the calculation at the quark level.

– A contribution [28,4] for isospin breaking occurs because of the mass difference between charged and neutral pions, which is essentially of electromagnetic origin. The spectral function has a kinematic factor β^3 which is different in e^+e^- ($\pi^+\pi^-$) and τ decay ($\pi^-\pi^0$). We write

$$v_0(s) = \frac{\beta_0^3(s)}{12}|F_\pi^0(s)|^2\ , \quad (18)$$

$$v_-(s) = \frac{\beta_-^3(s)}{12}|F_\pi^-(s)|^2\ , \quad (19)$$

Table 1. Expected sources of isospin symmetry breaking between e^+e^- and τ spectral functions in the 2π and 4π channels, and the corresponding corrections to $a_\mu^{\rm had,LO}$ as obtained from τ data. The corrections (I) follow essentially the procedure used in [4, 7,11], while in (II) the more complete approach of [30] is chosen. The values given for (II) differ slightly from those quoted in [30], because of the model used in the latter to parametrize the pion form factor, in addition to the re-evaluation of the short distance electroweak correction. The errors given are theoretical only. Uncertainties introduced by the experimental error on the τ spectral function itself are not accounted for here

Sources of Isospin Symmetry Breaking	$\Delta a_\mu^{\rm had,LO}$ (10^{-10}) $\pi^+\pi^-$ (I)	$\pi^+\pi^-$ (II)	$\pi^+\pi^-2\pi^0$	$2\pi^+2\pi^-$
Short distance rad. corr.	-10.3 ± 2.1	-12.1 ± 0.3	-0.36 ± 0.07	-0.18 ± 0.04
Long distance rad. corr.		-1.0		
$m_{\pi^-} \neq m_{\pi^0}$ (β in cross section)	-7.0	-7.0	$+0.6 \pm 0.6$	-0.4 ± 0.4
$m_{\pi^-} \neq m_{\pi^0}$ (β in ρ width)	$+4.2$	$+4.2$	–	–
$m_{\rho^-} \neq m_{\rho^0}$	0 ± 0.2	0 ± 2.0	–	–
$\rho - \omega$ interference	$+3.5 \pm 0.6$	$+3.5 \pm 0.6$	–	–
Electromagnetic decay modes	-1.4 ± 1.2	-1.4 ± 1.2	–	–
Sum	-11.0 ± 2.5	-13.8 ± 2.4	$+0.2 \pm 0.6$	-0.6 ± 0.4

with obvious notations, $F_\pi^{0,-}(s)$ being the electromagnetic and weak pion form factors, respectively, and $\beta_{0,-}$ defined by

$$\beta_{0,-} = \beta(s, m_{\pi^-}, m_{\pi^{0,-}}) \ , \qquad (20)$$

where

$$\beta(s, m_1, m_2) = \left[\left(1 - \frac{(m_1+m_2)^2}{s}\right) \times \left(1 - \frac{(m_1-m_2)^2}{s}\right)\right]^{1/2} . \qquad (21)$$

Hence, a correction equal to $\beta_0^3(s)/\beta_-^3(s)$ is applied to the τ spectral function.

– Other corrections occur in the form factor itself. It turns out that it is affected by the pion mass difference because the same β^3 factor enters in the $\rho \to \pi\pi$ width. This effect partially compensates the β^3 corrections (18), (19) of the cross section, as seen in Table 1.
– Similarly a possible mass difference between the charged and neutral ρ meson affects the value of the corresponding width and shifts the resonance lineshape. Theoretical estimates [119] and experimental determinations [5,120] show that the mass difference is compatible with zero within about 1 MeV.
– $\rho - \omega$ interference occurs in the $\pi^+\pi^-$ mode and thus represents an obvious source of isospin symmetry breaking. Its contribution can be readily introduced into the τ spectral function using the parameters determined in the CMD-2 fit [22]. The integral over the interference almost vanishes by itself since it changes sign at the ω mass, however the s-dependent integration kernel produces a net effect (Table 1).
– Electromagnetic ρ decays explicitly break SU(2) symmetry. This is the case for the decays $\rho \to \pi\pi^0\gamma$ through an ω intermediate state because of identical π^0's, $\rho \to \pi\gamma$, $\rho^0 \to \eta\gamma$ and $\rho^0 \to l^+l^-$. The decay $\rho \to \pi\pi\gamma$ deserves particular attention: calculations have been done with an effective model [121] for both charged and neutral ρ's. The different contributions are listed in Table 1.
– A breakdown of CVC is due to quark mass effects: m_u different from m_d generates $\partial_\mu J^\mu \sim (m_u - m_d)$ for a charge-changing hadronic current J^μ between u and d quarks. Expected deviations from CVC due to so-called second class currents such as, e.g., the decay $\tau^- \to \nu_\tau\pi^-\eta$ where the corresponding e^+e^- final state $\pi^0\eta$ (C=+1) is forbidden, lead to an estimated branching fraction of the order of $(m_u - m_d)^2/m_\tau^2 \simeq 10^{-5}$ [122], while the experimental upper limit amounts to $B(\tau \to \nu_\tau\pi^-\eta) < 1.4\ 10^{-4}$ [105].

5.2 A more elaborate treatment of isospin breaking in the 2π channel

The above analysis of isospin breaking leaves out the possibility of sizeable contributions from virtual loops. This problem was studied recently [29] within a model based on Chiral Perturbation Theory. In this way the correct low-energy hadronic structure is implemented and a consistent framework can be set up to calculate electroweak and strong processes, such as the radiative corrections in the $\tau \to \nu_\tau\pi^-\pi^0$ decay. One might worry that the ρ mass is too large for such a low-energy approach. However a reasonable matching with the resonance region [123] and even beyond is claimed to be achieved, providing a very useful tool to study radiative decays.

A new analysis has been issued [30] which is more suited to our purpose, in the sense that it applies to the inclusive radiative rate, $\tau \to \nu_\tau\,\pi^-\pi^0\,(\gamma)$, as measured by

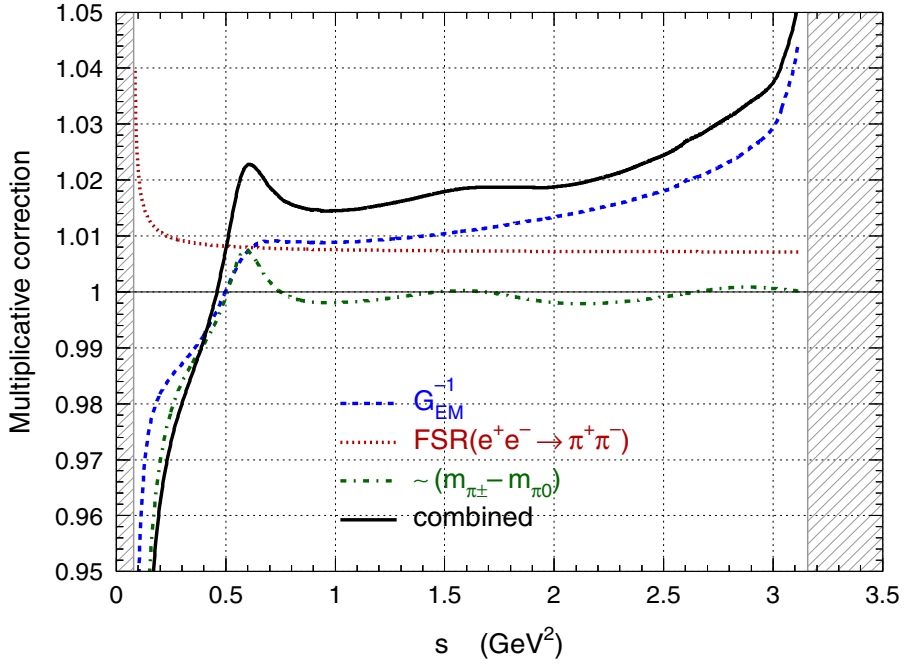

Fig. 4. Mass-squared-dependent corrections applied to the $\pi^-\pi^0$ spectral function from τ data, following the analysis of [30]

the experiments. A consistent calculation of radiative corrections is presented including real photon emission and the effect of virtual loops. All the contributions listed in the previous section are included and the isospin-breaking contributions in the pion form factor are now more complete. Following [30], the relation between the Born level e^+e^- spectral function and the τ spectral function (19) reads

$$v_{\pi^+\pi^-}(s) = \frac{1}{G_{\rm EM}(s)} \frac{\beta_0^3}{\beta_-^3} \left| \frac{F_\pi^0(s)}{F_\pi^-(s)} \right|^2 v_{\pi^-\pi^0(\gamma)}(s) \ , \quad (22)$$

where $G_{\rm EM}(s)$ is the long-distance radiative correction involving both real photon emission and virtual loops (the infrared divergence cancels in the sum). Note that the short-distance $S_{\rm EW}$ correction, discussed above, is already applied in the definition of $v_-(s)$ (*cf.* (10)), but its value differs from (17) because subleading quark-level and hadron-level contributions should not be added, as double counting would occur. The correct expression for the $\pi\pi^0$ mode therefore reads

$$S_{\rm EW}^{\pi\pi^0}(s) = \frac{S_{\rm EW}^{\rm had} G_{\rm EM}(s)}{S_{\rm EW}^{\rm sub,lep}} = (1.0233 \pm 0.0006) \cdot G_{\rm EM}(s) \ , \quad (23)$$

the subleading hadronic corrections being now incorporated in the mass-dependent $G_{\rm EM}(s)$ factor. The form factor correction is dominated by the effect of the pion mass difference in the ρ width, but it also includes a small contribution at the 10^{-3} level from the 'chiral' form used for the ρ lineshape. In practice, however, the correction is independent of the chosen parametrization of the form factor. The different contributions to the isospin-breaking corrections are shown in the second column of Table 1. The values slightly differ from those given in [30] because the authors use a model for the pion form factor rather than integrating experimental data. The largest difference however stems from our re-evaluation of the short-distance electroweak correction, $S_{\rm EW}$, including the subleading leptonic contribution. The sum amounts to $(-13.8\pm2.4)10^{-10}$ to be compared with $(-12.0\pm2.6)10^{-10}$ given in [30].

The dominant uncertainty in this method stems from the $\rho^\pm$-ρ^0 mass difference. Indeed, in the chiral model used in [30] the only parameter entering the pion form factor is the ρ mass, since the width is given by $\Gamma_\rho(s) = m_\rho s\,\beta^3(s)/(96\pi f_\pi^2)$. In the method previously used and recalled in Sect. 5.1, the width at the pole was taken as an independent parameter with

$$\Gamma_\rho(s) = \Gamma_\rho \sqrt{s}\,\beta^3(s)/(m_\rho \beta^3(m_\rho^2)),$$

so that the effect of the ρ mass difference approximately cancels after integration. This explains the large difference in the uncertainties quoted for the two evaluations in Table 1.

Since the integral (5) requires as input the e^+e^- spectral function including FSR photon emission, a final correction is necessary. It is identical to that applied in the CMD-2 analysis [22,111] (cf. Sect. 4). All the corrections are drawn versus s in Fig. 4. The overall correction reduces the τ rate below the ρ peak, but, somewhat unexpectedly, has the opposite effect above. This behavior is driven by the long-distance radiative corrections contained in $G_{\rm EM}(s)$.

The total correction to the τ result in this method, not including the FSR contribution, amounts to $\Delta a_\mu^{\rm had} = (-13.8 \pm 2.4)\ 10^{-10}$, where the main contribution to the error is due to the experimental limits on the ρ mass difference. After including the FSR contribution, it becomes $(-9.3 \pm 2.4)\ 10^{-10}$, a value consistent with the result in

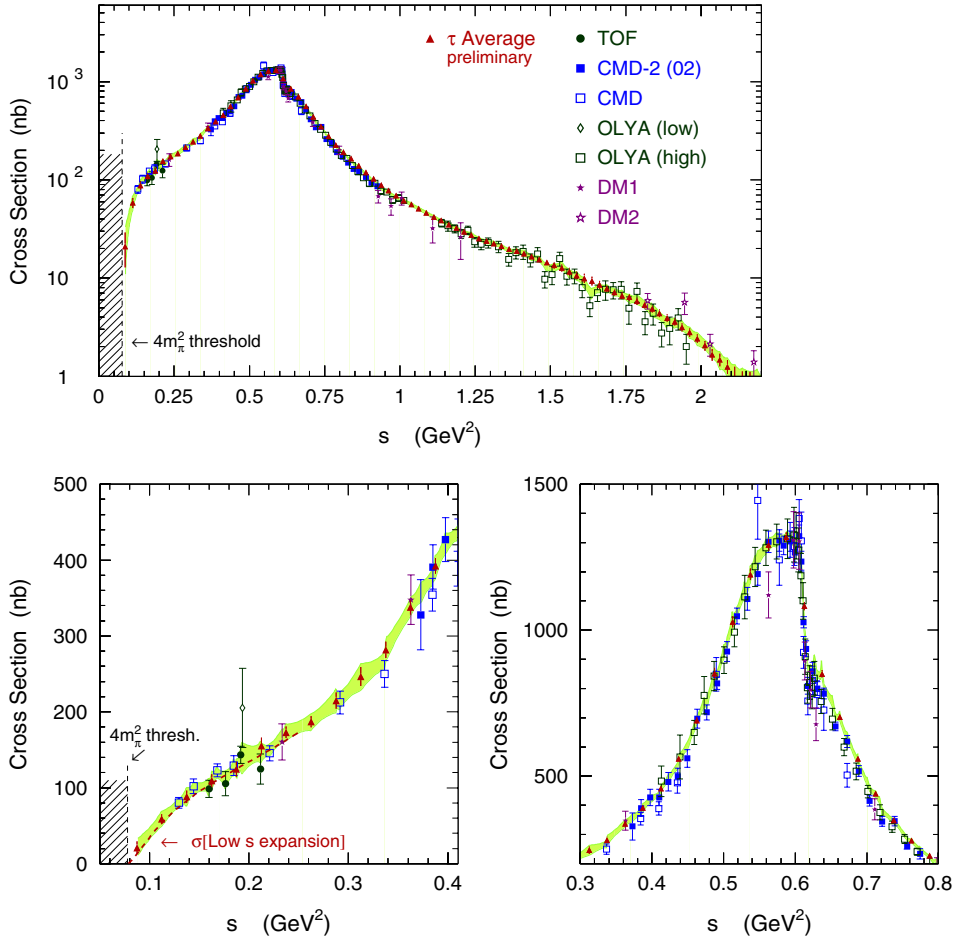

Fig. 5. Comparison of the $\pi^+\pi^-$ spectral functions from e^+e^- and isospin-breaking corrected τ data, expressed as e^+e^- cross sections. The band indicates the combined e^+e^- and τ result within 1σ errors. It is given for illustration purpose only

the first column of Table 1 which does not include the virtual corrections and uses a less sophisticated treatment of radiative decays. In the following we apply the correction functions from the more complete analysis (method (II) in Table 1) and keep the corresponding uncertainty separate from the purely experimental errors.

5.3 Isospin breaking in 4π channels

There exists no comparable study of isospin breaking in the 4π channels. Only kinematic corrections resulting from the pion mass difference have been considered so far [28], which we have applied in this analysis. It creates shifts of $-0.7\ 10^{-10}$ (-3.8%) and $+0.1\ 10^{-10}$ ($+1.1\%$) for $2\pi^+2\pi^-$ and $\pi^+\pi^-2\pi^0$, respectively. However, since the four-pion contribution to $a_\mu^{\rm had,LO}$ is relatively less important than the two-pion part (by a little more than an order of magnitude in the integration range up to 1.8 GeV) and the experimental uncertainties are much larger, we feel this is a justified procedure at the present level of accuracy of the data. Moreover, the entire correction has been attributed as systematic error which is kept separate from the experimental errors on $a_\mu^{\rm had,LO}$ from these channels.

It should also be pointed out that the systematic uncertainties from isospin breaking are essentially uncorrelated between the 2π and 4π modes: as Table 1 shows, the dominant sources of uncertainties are the $\rho^\pm$-ρ^0 mass difference for 2π and the threshold factors in 4π where large errors have been given to cover uncertainties in the decay dynamics and the missing pieces.

6 Comparison of e^+e^- and τ spectral functions

The e^+e^- and the isospin-breaking corrected τ spectral functions can be directly compared for the dominant 2π and 4π final states. For the 2π channel, the ρ-dominated form factor falls off very rapidly at high energy so that the comparison can be performed in practice over the full energy range of interest. The situation is different for the 4π channels where the τ decay kinematics limits the exercise to energies less than ~ 1.6 GeV, with only limited statistics beyond.

6.1 Direct comparison

Figure 5 shows the comparison for the 2π spectral functions. Visually, the agreement seems satisfactory, however the large dynamical range involved does not permit an accurate test. To do so, the e^+e^- data are plotted as a

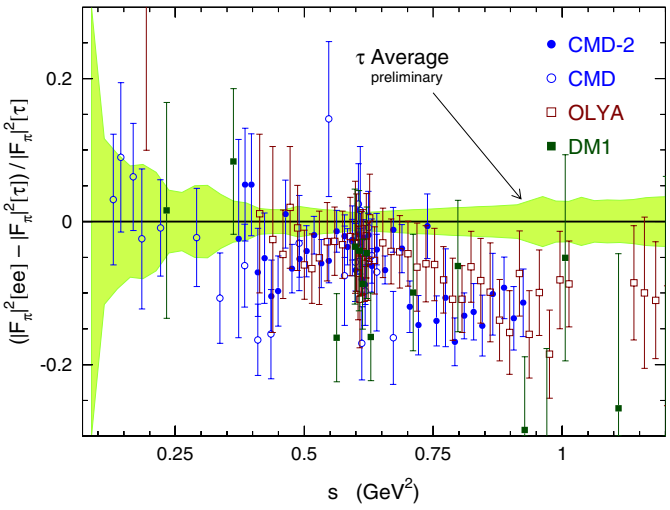

Fig. 6. Relative comparison of the $\pi^+\pi^-$ spectral functions from e^+e^- and isospin-breaking corrected τ data, expressed as a ratio to the τ spectral function. The band shows the uncertainty on the latter

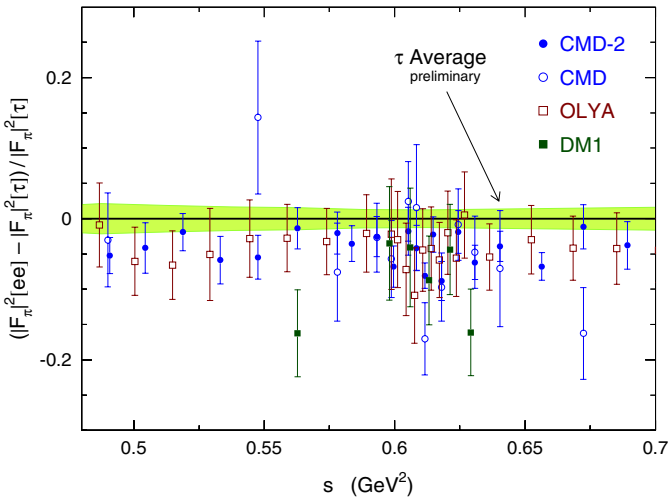

Fig. 7. Relative comparison in the ρ region of the $\pi^+\pi^-$ spectral functions from e^+e^- and isospin-breaking corrected τ data, expressed as a ratio to the τ spectral function. The band shows the uncertainty on the latter

point-by-point ratio to the τ spectral function in Fig. 6, and enlarged in Fig. 7, to better emphasize the region of the ρ peak[3]. The e^+e^- data are significantly lower by 2-3% below the peak, the discrepancy increasing to about 10% in the 0.9-1.0 GeV region.

The comparison for the 4π cross sections is given in Fig. 8 for the $2\pi^+2\pi^-$ channel and in Fig. 9 for $\pi^+\pi^-2\pi^0$. As noted before, the latter suffers from large differences between the results from the different e^+e^- experiments. The τ data, combining two measured spectral functions according to (9) and corrected for isospin breaking as discussed in Sect. 5, lie somewhat in between with large uncertainties above 1.4 GeV because of the lack of statistics and a large feedthrough background in the $\tau \to \nu_\tau\, \pi^- 3\pi^0$ mode. In spite of these difficulties the $\pi^- 3\pi^0$ spectral function is in agreement with e^+e^- data as can be seen in Fig. 8. It is clear that intrinsic discrepancies exist among the e^+e^- experiments and that a quantitative test of CVC in the $\pi^+\pi^-2\pi^0$ channel is premature.

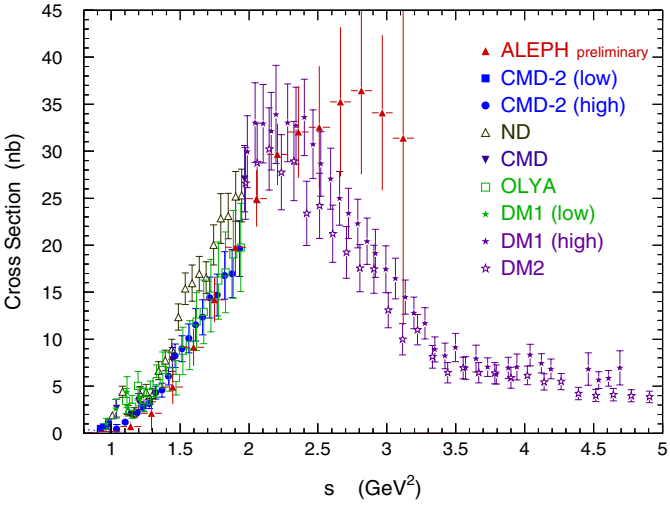

Fig. 8. Comparison of the $2\pi^+2\pi^-$ spectral functions from e^+e^- and isospin-breaking corrected τ data, expressed as e^+e^- cross sections

6.2 Branching ratios in τ decays and CVC

A convenient way to assess the compatibility between e^+e^- and τ spectral functions proceeds with the evaluation of τ decay fractions using the relevant e^+e^- spectral functions as input. All the isospin-breaking corrections detailed in Sect. 5.2 are included. The advantage of this procedure is to allow a quantitative comparison using a single number. The weighting of the spectral function is however different from the vacuum polarization kernels. Using the branching fraction $B(\tau^- \to \nu_\tau\, e^-\, \bar{\nu}_e) =$ (17.810±0.039)%, obtained assuming leptonic universality in the charged weak current [24], the results for the main channels are given in Table 2. The errors quoted for the CVC values are split into uncertainties from (*i*) the experimental input (the e^+e^- annihilation cross sections) and the numerical integration procedure, (*ii*) the missing radiative corrections applied to the relevant e^+e^- data, and (*iii*) the isospin-breaking corrections when relating τ and e^+e^- spectral functions. The values for the τ branching ratios involve measurements [24,124,125] given without charged hadron identification, i.e., for the $h\pi^0\nu_\tau$, $h3\pi^0\nu_\tau$ and $3h\pi^0\nu_\tau$ final states. The corresponding channels with charged kaons have been measured [126,127] and their contributions can be subtracted out in order to obtain the pure pionic modes.

[3] The central bands in Figs. 6 and 7 give the quadratic sum of the statistical and systematic errors of the combined τ spectral functions. Local bumps in these bands stem from increased errors when combining different experiments having local inconsistencies. We use the procedure described in Sect. 7.1

Table 2. Branching fractions of τ vector decays into 2 and 4 pions in the final state. Second column: world average. Third column: inferred from e^+e^- spectral functions using the isospin relations (7–9) and correcting for isospin breaking. The experimental error of the $\pi^+\pi^-$ CVC value contains an absolute procedural integration error of 0.08%. Experimental errors, including uncertainties on the integration procedure, and theoretical (missing radiative corrections for e^+e^-, and isospin-breaking corrections and V_{ud} for τ) are shown separately. Right column: differences between the direct measurements in τ decays and the CVC evaluations, where the separate errors have been added in quadrature

Mode	Branching fractions (in%)		
	τ data	e^+e^- via CVC	$\Delta(\tau - e^+e^-)$
$\tau^- \to \nu_\tau \pi^- \pi^0$	25.46 ± 0.12	$23.98 \pm \underbrace{0.25_{\rm exp} \pm 0.11_{\rm rad} \pm 0.12_{\rm SU(2)}}_{0.30}$	$+1.48 \pm 0.32$
$\tau^- \to \nu_\tau \pi^- 3\pi^0$	1.01 ± 0.08	$1.09 \pm \underbrace{0.06_{\rm exp} \pm 0.02_{\rm rad} \pm 0.05_{\rm SU(2)}}_{0.08}$	-0.08 ± 0.11
$\tau^- \to \nu_\tau 2\pi^- \pi^+ \pi^0$	4.54 ± 0.13	$3.63 \pm \underbrace{0.19_{\rm exp} \pm 0.04_{\rm rad} \pm 0.09_{\rm SU(2)}}_{0.21}$	$+0.91 \pm 0.25$

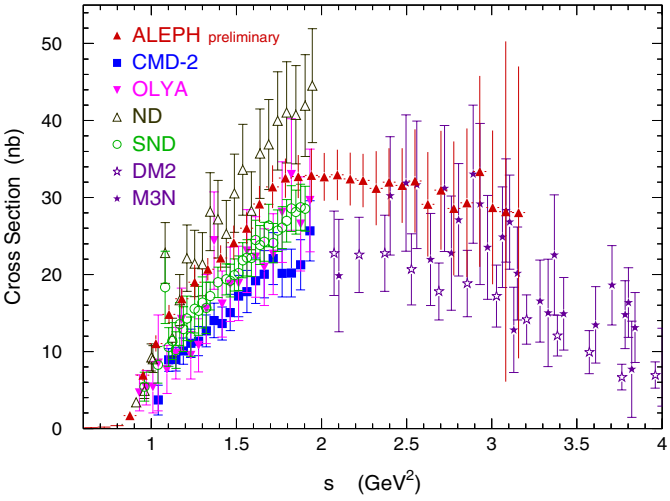

Fig. 9. Comparison of the $\pi^+\pi^-2\pi^0$ spectral functions from e^+e^- and isospin-breaking corrected τ data, expressed as e^+e^- cross sections

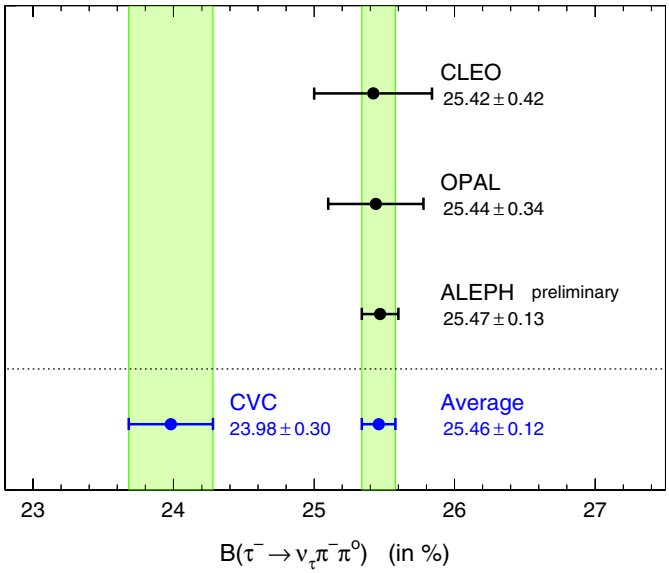

Fig. 10. The measured branching ratios for $\tau \to \nu_\tau \pi^- \pi^0$ compared to the prediction from the $e^+e^- \to \pi^+\pi^-$ spectral function applying the isospin-breaking correction factors discussed in Sect. 5.2. The measured branching ratios are from ALEPH [24], CLEO [124] and OPAL [125]. The OPAL result was obtained from their $h\pi^0$ branching ratio, reduced by the small $K\pi^0$ contribution measured by ALEPH [126] and CLEO [127]

As expected from the preceding discussion, a large discrepancy is observed for the $\tau \to \nu_\tau \pi^- \pi^0$ branching ratio, with a difference of $(-1.48 \pm 0.12_\tau \pm 0.25_{\rm ee} \pm 0.11_{\rm rad} \pm 0.12_{\rm SU(2)})\%$, where the uncertainties are from the τ branching ratio, e^+e^- cross sections, e^+e^- missing radiative corrections and isospin-breaking corrections (including the uncertainty on V_{ud}), respectively. Adding all errors in quadrature, the effect represents a 4.6 σ discrepancy. Since the disagreement between e^+e^- and τ spectral functions is more pronounced at energies above 750 MeV, we expect a smaller discrepancy in the calculation of $a_\mu^{\rm had,LO}$ because of the steeply falling kernel $K(s)$ in this case. More information on the comparison is displayed in Fig. 10 where it is clear that ALEPH, CLEO and OPAL all separately, but with different significance, disagree with the e^+e^--based CVC result.

The situation in the 4π channels is different. Agreement is observed for the $\pi^- 3\pi^0$ mode within an accuracy of 11%, however the comparison is not satisfactory for the $2\pi^-\pi^+\pi^0$ mode. In the latter case, the relative difference is very large, $(22 \pm 6)\%$, compared to any reasonable level of isospin symmetry breaking. As such, it rather points to experimental problems that have to be investigated.

7 The integration procedure

The information used for the evaluation of the integral (5) comes mainly from direct measurements of the cross sections in e^+e^- annihilation and via CVC from τ spectral

functions. In general, the integrals themselves are evaluated using the trapezoidal rule, i.e., combining adjacent measurement points by linear interpolation. Even if this method is straightforward and free from theoretical assumptions (other than CVC in the τ case), its numerical calculation requires special care. The finite and variable distance between adjacent measurements creates systematic uncertainties that have to be estimated. The combination of measurements from different experiments taking into account correlations – both within each data set and between different experiments – is the subject of additional discussions presented in the following.

7.1 Averaging data from different experiments

To exploit the maximum information from the available data, we combine weighted measurements of different experiments at a given energy instead of calculating separately the integrals for every experiment and finally averaging them.

The solution of the averaging problem is found by minimizing

$$\chi^2 \;=\; \sum_{n=1}^{N_{exp}} \sum_{i,j=1}^{N_n} (x_i^n - k_i)\,(C_{ij}^n)^{-1}\,(x_j^n - k_j)\;, \qquad (24)$$

where x_i^n is the ith cross section measurement of the nth experiment in a given final state, C_{ij}^n is the covariance between the ith and the jth measurement and k_i is the unknown distribution to be determined. The covariance matrix C^n is given by

$$C_{ij}^n = \begin{cases} (\Delta_{i,stat}^n)^2 + (\Delta_{i,sys}^n)^2 & for\ i = j \\ \Delta_{i,sys}^n \cdot \Delta_{j,sys}^n & for\ i \neq j \end{cases}\;, \quad i,j = 1,\ldots,N_n\;, \qquad (25)$$

where $\Delta_{i,stat}^n$ ($\Delta_{i,sys}^n$) denotes the statistical (systematic) error of x_i^n. The systematic errors of the e^+e^- annihilation measurements are essentially due to luminosity and efficiency uncertainties. It is conservative to take them as common errors of all data points of a given experiment. The minimum condition $d\chi^2/dk_i = 0,\ \forall i$ leads to the system of linear equations

$$\sum_{n=1}^{N_{exp}} \sum_{j=1}^{N_n} (x_j^n - k_j)\,(C_{ij}^n)^{-1} \;=\; 0\;, \quad i = 1,\ldots,N_n\;. \qquad (26)$$

The inverse covariance $\tilde{C}_{ij}^{-1}$ between the solutions k_i, k_j is the sum of the inverse covariances of each experiment

$$\tilde{C}_{ij}^{-1} \;=\; \sum_{n=1}^{N_{exp}} (C_{ij}^n)^{-1}\;. \qquad (27)$$

If different measurements at a given energy show inconsistencies, i.e., their χ^2 per number of degrees of freedom (DF) is larger than one, we rescale the error of their weighted average by $\sqrt{\chi^2/\mathrm{DF}}$.

7.2 Correlations between experiments

Equation (27) provides the covariance matrix needed for the error propagation when calculating the integrals over the solutions k_i from (26). Up to this point, $\tilde{C}_{ij}$ only contains correlations between the systematic uncertainties within the same experiment. However, due to commonly used simulation techniques for the acceptance and luminosity determination as well as state-of-the-art calculations of radiative corrections, systematic correlations from one experiment to another occur. It is obviously a difficult task to reasonably estimate the amount of such correlations as they depend on the reconstruction capabilities of the experiments and the theoretical understanding of the underlying decay dynamics. In general, one can state that in older experiments, where only parts of the total solid angle were covered by the detector acceptance, individual experimental limitations should dominate the systematic uncertainties. Potentially common systematics, such as radiative corrections or efficiency, acceptance and luminosity calculations based on the Monte Carlo simulation, play only minor roles. The correlations between systematic errors below 2 GeV energy are therefore estimated to be between 10% and 30%, with the exception of the $\pi^+\pi^-$ final state, where we impose a 40% correlation due to the simpler experimental situation and the better knowledge of the dynamics which leads to non-negligible systematic contributions from the uncertainties of the radiative corrections. At energies above 2 GeV the experiments measured the total inclusive cross section ratio R. Between 2 and 3 GeV, individual technical problems dominate the systematic uncertainties. At higher energies, new experiments provide nearly full geometrical acceptance which decreases the uncertainty of efficiency estimations. Radiative corrections as well as theoretical errors of the luminosity determination give important contributions to the final systematic errors quoted by the experiments. We therefore estimate the correlations between the systematic errors of the experiments to be negligible between 2 GeV and 3 GeV, 20% between 3 GeV and 10 GeV. These correlation coefficients are added to all those entries of $\tilde{C}_{ij}$ from (27) which involve two different experiments.

7.3 Evaluation of the integral

The procedure described above provides the weighted average and the covariance of the cross sections from different experiments contributing to a certain final state in a given range of energies. We now apply the trapezoidal rule. To perform the integration (5), we subdivide the integration range in fine energy steps and calculate for each of these steps the corresponding covariance (where additional correlations induced by the trapezoidal rule have to be taken into account). This procedure yields error envelopes between adjacent measurements as depicted by the shaded bands in the corresponding figures.

As a cross check, a different procedure of the evaluation of the integral has been applied. For each final state, results of different experiments contributing to it in a given

Table 3. Fit results of the low energy expansion (29) to e^+e^- and τ data, the latter corrected for SU(2) breaking. The right column quotes the contributions to $a_\mu^{\rm had,LO}$, integrated from threshold to 0.5 GeV. The errors are dominated by experiment, but take into account systematic uncertainties from the fitting procedure (mainly the variation of the upper energy cut yielding, e.g., an uncertainty of about $0.49\,10^{-10}$ for τ data). The systematics in $a_\mu^{\rm had,LO}$ from radiative corrections (e^+e^-) and isospin breaking (τ) (cf. Sects. 4, 5.1) are quoted apart

Data	Coefficient	Fit result	Correlation matrix			$a_\mu^{\rm had,LO}$ (10^{-10}) $[2m_{\pi^\pm} - 0.5$ GeV$]$
	$\langle r^2\rangle_\pi$	(0.439 ± 0.008) fm^2	1	$\star$	$\star$	
e^+e^-	c_1	(6.8 ± 1.9) GeV^{-4}	-0.15	1	$\star$	$58.0 \pm 1.7 \pm 1.1_{\rm rad}$
	c_2	(-0.7 ± 6.8) GeV^{-6}	0.09	-0.97	1	
	$\langle r^2\rangle_\pi$	(0.439 ± 0.008) fm^2	1	$\star$	$\star$	
τ	c_1	(3.3 ± 1.7) GeV^{-4}	-0.15	1	$\star$	$56.0 \pm 1.6 \pm 0.3_{\rm SU(2)}$
	c_2	(13.2 ± 5.7) GeV^{-6}	0.09	-0.99	1	

energy range are integrated separately using a rectangular method. After that a weighted average, based on the statistical and systematic errors combined in quadrature, is calculated. In some cases when correlations between systematic uncertainties of different experiments are known, they are taken into account after averaging the results with weights based on the statistical errors only. As mentioned above, if results of the integration for different measurements are found to be inconsistent, the error is rescaled by a factor $\sqrt{\chi^2/{\rm DF}}$.

The difference between the results of the two described procedures is considered when estimating the systematic uncertainty on the numerical integration procedure. The systematics also take into account variations of the energy interval where several data points are lumped into a single value, and the effect on the central value of the integral when including or not the correlations. The procedural systematics are added in quadrature to the experimental error on the integral. For instance, in the case of the $\pi^+\pi^-$ contribution, this procedural uncertainty amounts to 1.5 10^{-10}.

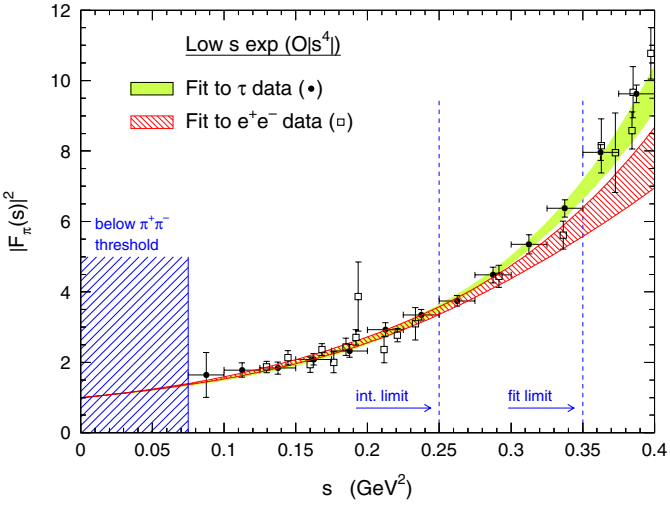

Fig. 11. Fit of the pion form factor from $4m_\pi^2$ to 0.35 GeV^2 using a third-order Taylor expansion with the constraints at $s = 0$ and the measured pion r.m.s. charge radius from space-like data [128]. The result of the fit is integrated only up to 0.25 GeV^2

8 Specific contributions

In some energy regions where data information is scarce and reliable theoretical predictions are available, we use analytical contributions to extend the experimental integral. Also, the treatment of narrow resonances involves a specific procedure.

8.1 The $\pi^+\pi^-$ threshold region

To overcome the lack of precise data at threshold energies and to benefit from the analyticity property of the pion form factor, a third order expansion in s is used. The pion form factor F_π^0 is connected with the $\pi^+\pi^-$ cross section via the expression

$$|F_\pi^0|^2 \;=\; \frac{3s}{\pi\alpha^2\beta_0^3}\;\sigma_{\pi\pi}\;. \qquad (28)$$

The expansion for small s reads

$$F_\pi^0 \;=\; 1 + \frac{1}{6}\langle r^2\rangle_\pi\, s + c_1\, s^2 + c_2\, s^3 + O(s^4)\;. \qquad (29)$$

Exploiting precise results from space-like data [128], the pion charge radius-squared is constrained to $\langle r^2\rangle_\pi = (0.439 \pm 0.008)$ fm^2 and the two parameters $c_{1,2}$ are fitted to the data in the range $[2m_\pi$, 0.6 GeV$]$. In the case of τ data, isospin corrections are taken into account as discussed before.

The results of the fits are given in Table 3 and shown in Fig. 11. Good agreement is observed in the low energy region where the expansion should be reliable. Since the fits incorporate unquestionable constraints from first principles, we have chosen to use this parameterization for evaluating the integrals in the range up to 0.5 GeV. Systematic uncertainties due to the fitting procedure (fit boundaries,

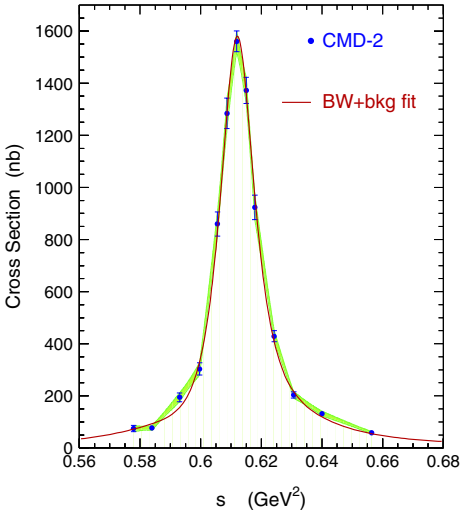

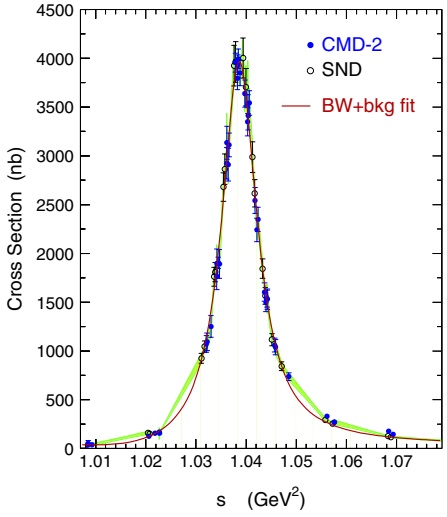

Fig. 12. Cross sections of the ω (*left*) and ϕ (*right*) resonances. The dots with error bars depict the measurements, the shaded band is the result of the trapezoidal rule within (correlated) errors and the function shows the phenomenological fit of a BW resonance plus one (ω) or two (ϕ) Gaussians to account for other than the single resonance contributions. The bias of the trapezoidal rule when applied to a strongly concave (or convex) distribution is particularly visible in the tails of the ϕ resonance when comparing to the BW fit. It leads to an overestimation of the integral

whether or not the coefficient c_2 is fixed) are small, albeit taken into account.

8.2 Integration over the ω and ϕ resonances

In the regions around the ω and ϕ resonances we have assumed in the preceding works that the cross section of the $\pi^+\pi^-\pi^0$ production on the one hand, and the $\pi^+\pi^-\pi^0$, K^+K^- as well as $K^0_SK^0_L$ production on the other hand is saturated by the corresponding resonance production. In a data driven approach it is however more careful to directly integrate the measurement points without introducing prior assumptions on the underlying process dynamics [129]. Possible non-resonant contributions and interference effects are thus accounted for.

Notwithstanding, a straightforward trapezoidal integration buries the danger of a bias: with insufficient scan density, the linear interpolation of the measurements leads to a significant overestimation of the integral when dealing with strongly concave functions such as the tails of Breit-Wigner resonance curves. This effect is particularly visible in the right hand plot of Fig. 12, showing the ϕ resonance: the cross sections are measured by SND [46] (sum of the final states K^+K^-, $K^0_SK^0_L$ and $\pi^+\pi^-\pi^0$ and corrected for missing modes, i.e., rescaled by $(0.984 \pm 0.009)^{-1}$ [105]) and CMD-2 [48] ($K^0_SK^0_L$ only, rescaled by $(0.337\pm0.005)^{-1}$ [105]). Shown in addition are the error band of the trapezoidal rule and the solution of a phenomenological fit of a BW resonance plus two Gaussians (only one Gaussian is necessary for the ω, see left hand plot in Fig. 12) to account for contributions other than the single resonance. Both fits result in satisfactory χ^2 values. Since we are only interested in the integral and do not want to extract dynamical parameters like phases or branching fractions, it is not necessary to parametrize the exact structure of the physical processes. We have accounted for the systematics due to the arbitrariness in the choice of the parametrization by varying the functions and parameters used. The resulting effects are numerically small compared to the experimental errors (see Table 4). It is clear from Fig. 12 that the fit function passes below the trapezoidal bands in the concave tails of both the ϕ and the ω.

Table 4 gives the contributions to $a_\mu^{\rm had,LO}$ from the different energy domains covered by the experiments for both the ω and the ϕ. Since the experiments quote the cross section results without correcting for leptonic and hadronic vacuum polarization in the photon propagator (cf. the discussion in Sect. 4), we perform the correction here. Note that the data shown in Fig. 12 have been corrected for vacuum polarization. A small FSR correction (cf. Sect. 4) is applied to the results given in Table 4. The correction of hadronic vacuum polarization being iterative and thus only approximative, we assign half of the total vacuum polarization correction as generous systematic errors (cf. Sect. 4). In spite of that, the evaluation of $a_\mu^{\rm had,LO}$ is dominated by the experimental uncertainties. Since the trapezoidal rule is biased, we choose the results based on the BW fits for the final evaluation of $a_\mu^{\rm had,LO}$.

8.3 Narrow $c\bar{c}$ and $b\bar{b}$ resonances

The contributions from the narrow J/ψ resonances are computed using a relativistic Breit-Wigner parametrization for their line shape. The physical values for the resonance parameters and their errors are taken from the latest compilation in [105]. Vacuum polarization effects are already included in the quoted leptonic widths. The total parametrization errors are then calculated by Gaussian error propagation. This integration procedure is not followed for the $\psi(3S)$ state which is already included in the R measurements, and for the Υ resonances which are represented in an average sense (global quark-hadron duality) by the $b\bar{b}$ QCD contribution, discussed next.

8.4 QCD prediction at high energy

Since the emphasis in this paper is on a complete and critical evaluation of spectral functions from low-energy data, we have adopted the conservative choice of using

Table 4. Contributions to $a_\mu^{\rm had,LO}$ from the narrow resonances $\omega(782)$ (upper table) and $\phi(1020)$ (lower table). Given are the results for the BW fit (first column) and the trapezoidal rule (second column). The next three columns quote the experimental errors, the fit parameterization systematics and the uncertainty introduced by the correction for the missing decay modes of the resonances. The energy interval of the integration and the integration type (data or analytical function) are given in the last two columns. Systematic errors from the same sources, but for different energy regions are added linearly in the sum. All other errors are added in quadrature, the total errors being labelled 'tot'. Additional systematics are due to the vacuum polarization (VP) correction, taken to be half of the full correction, and to final state radiation (FSR) where the full correction is accounted as uncertain

$a_\mu^{\rm had,LO}$ (10^{10})		$\sigma(a_\mu^{\rm had,LO})$ (10^{10})			Energy range	Type/Ref
BW Fit	Trapez.	Exp.	Fit	BR	(GeV)	
$\boldsymbol{\omega}$						
34.42	35.45	0.63	0.37	0.27	0.760184 - 0.810	CMD-2 [47]
2.51	-	0.06	0.30	0.02	0.300 - 0.760184	BW fit
36.94	37.96	$0.84_{\rm tot} \pm 0.73_{\rm VP} \pm 0.30_{\rm FSR}$			0.300 - 0.810	Sum
$\boldsymbol{\phi}$						
33.42	34.89	1.72	0.37	0.30	1.01017 - 1.03948	SND [46]
32.84	34.28	0.72	0.39	0.49	1.01017 - 1.03948	CMD-2 [48]
32.93	34.37	$0.91_{\rm tot}$			1.01017 - 1.03948	Average
0.77	-	0.02	0.07	0.01	1 - 1.01017	BW fit
-	1.10	0.06	0.01	0.01	1.03948 - 1.055	SND [46]
34.80	36.24	$0.92_{\rm tot} \pm 0.63_{\rm VP} \pm 0.14_{\rm FSR}$			1 - 1.055	Sum

the QCD prediction only above an energy of 5 GeV. The details of the calculation can be found in our earlier publications [7,11] and in the references therein. Only a very brief summary shall be given here.

The perturbative QCD prediction uses a next-to-next-to-leading order $O(\alpha_s^3)$ expansion of the Adler D-function [130], with second-order quark mass corrections included [131]. $R(s)$ is obtained by evaluating numerically a contour integral in the complex s plane. Nonperturbative effects are considered through the Operator Product Expansion, giving power corrections controlled by gluon and quark condensates. The value $\alpha_s(M_Z^2) = 0.1193 \pm 0.0026$, used for the evaluation of the perturbative part, is taken as the average of the results from the analyses of τ decays [6] and of the Z width in the global electroweak fit [132]. The two determinations have comparable uncertainties (mostly theoretical for the τ and experimental for the Z) and agree well with each other. We conservatively take as final uncertainty the value quoted in either analysis. As for the other contributions, uncertainties are taken to be equal to half of the quark mass corrections and to the full nonperturbative contributions.

A test of the QCD prediction can be performed in the energy range between 1.8 and 3.7 GeV. The contribution to $a_\mu^{\rm had,LO}$ in this region is computed to be $(33.87 \pm 0.46)\ 10^{-10}$ using QCD, to be compared with the result, $(34.9 \pm 1.8)\ 10^{-10}$ from the data. The two values agree within the 5% accuracy of the measurements.

In [11] the evaluation of $a_\mu^{\rm had,LO}$ was shown to be improved by applying QCD sum rules. We do not consider this possibility in the present analysis for the following two reasons. First, it is clear that the main problem at energies below 2 GeV is now the inconsistency between the e^+e^- and τ input data, and this must be resolved with priority. Second, the improvement provided by the use of QCD sum rules results from a balance between the experimental accuracy of the data and the theoretical uncertainties. The present precision of both e^+e^- and τ data, should they agree, is such that the gain would be smaller than before. This state of affairs will be reconsidered when the problems with the input data are sorted out.

9 Results

9.1 Lowest order hadronic contributions

Before adding up all the contributions to $a_\mu^{\rm had,LO}$, we shall summarize the procedure. On the one hand, the e^+e^--based evaluation is done in three pieces: the sum of exclusive channels below 2 GeV, the R measurements in the 2-5 GeV range and the QCD prediction for R above. Major contributions stem from the 2π (73%) and the two 4π (4.5%) channels. On the other hand, in the τ-based evaluation, the latter three contributions are taken from τ data up to 1.6 GeV and complemented by e^+e^- data above, because the τ spectral functions run out of precision near the kinematic limit of the τ mass. Thus, for nearly 77% of $a_\mu^{\rm had,LO}$ (contributing 80% of the total error-squared), two independent evaluations (e^+e^- and τ) are produced,

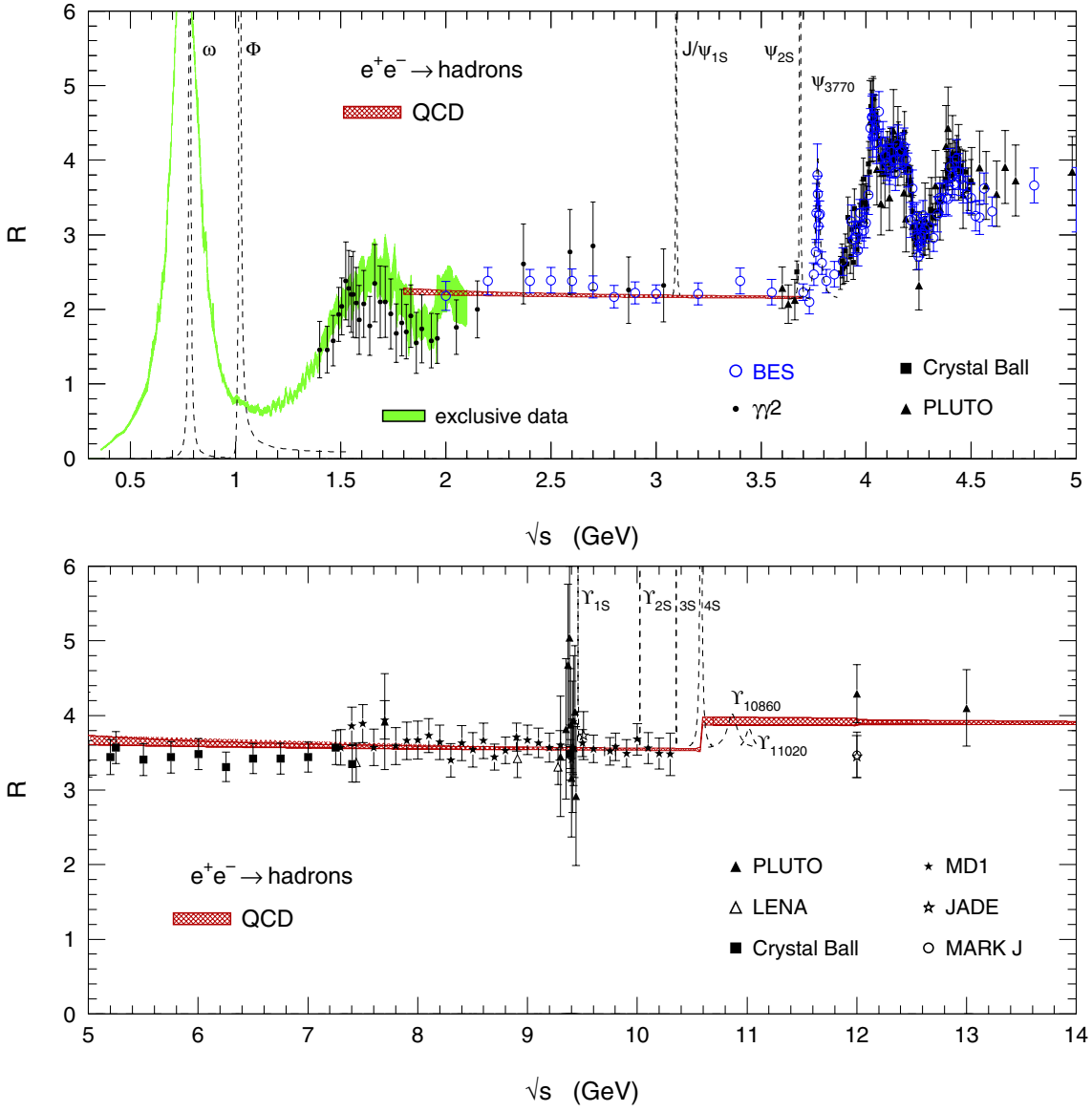

Fig. 13. Compilation of the data contributing to $a_\mu^{\rm had,LO}$. Shown is the total hadronic over muonic cross section ratio R. The shaded band below 2 GeV represents the sum of the exclusive channels considered in this analysis, with the exception of the contributions from the narrow resonances which are given as dashed lines. All data points shown correspond to inclusive measurements. The cross-hatched band gives the prediction from (essentially) perturbative QCD, which is found to be in good agreement with the measurements in the continuum above 2 GeV. In this figure the $b\bar{b}$ threshold is indicated at the onset of $B\overline{B}$ states in order to facilitate the comparison with data in the continuum. In the actual calculation the threshold is taken at twice the pole mass of the b quark

the remainder being computed from e^+e^- data and QCD alone.

Figure 13 gives a panoramic view of the e^+e^- data in the relevant energy range. The shaded band below 2 GeV represents the sum of the exclusive channels considered in the analysis. It turns out to be smaller than our previous estimate [4], essentially because more complete data sets are used and new information on the dynamics could be incorporated in the isospin constraints for the missing channels. It should be pointed out that the exclusive sum could lead to an underestimation of R, as some unmeasured higher multiplicity hadronic channels could start to play a role in the 2 GeV region. Nevertheless, good agreement is observed at 2 GeV with the first inclusive data point from BES, thus indicating that the missing component is likely to be small. The QCD prediction is indicated by the cross-hatched band. It is used in this analysis only for energies above 5 GeV. Note that the QCD band is plotted taking into account the thresholds for open flavour B states, in order to facilitate the comparison with the data in the continuum. However, for the evaluation of the integral, the $b\bar{b}$ threshold is taken at twice the pole mass of the b quark, so that the contribution includes the narrow Υ resonances, according to global quark-hadron duality.

Table 5. Summary of the $a_\mu^{\rm had,LO}$ contributions from e^+e^- annihilation and τ decays. The uncertainties on the vacuum polarization and FSR corrections are given as second errors in the individual e^+e^- contributions, while those from isospin breaking are similarly given for the τ contributions. These 'theoretical' uncertainties are correlated among all channels, except in the case of isospin breaking which shows little correlation between the 2π and 4π channels. The errors given for the sums in the last line are from the experiment, the missing radiative corrections in e^+e^- and, in addition for τ, SU(2) breaking

Modes	Energy [GeV]	$a_\mu^{\rm had,LO}$ (10^{-10}) e^+e^-	τ [3]	$\Delta(e^+e^- - \tau)$
Low s exp. $\pi^+\pi^-$	$[2m_{\pi^\pm} - 0.500]$	$58.04 \pm 1.70 \pm 1.14$	$56.03 \pm 1.61 \pm 0.28$	$+2.0 \pm 2.6$
$\pi^+\pi^-$	$[0.500 - 1.800]$	$440.81 \pm 4.65 \pm 1.54$	$464.03 \pm 3.19 \pm 2.34$	-23.2 ± 6.3
$\pi^0\gamma$, $\eta\gamma$ [1]	$[0.500 - 1.800]$	$0.93 \pm 0.15 \pm 0.01$	-	-
ω	$[0.300 - 0.810]$	$36.94 \pm 0.84 \pm 0.80$	-	-
$\pi^+\pi^-\pi^0$ [below ϕ]	$[0.810 - 1.000]$	$4.20 \pm 0.40 \pm 0.05$	-	-
ϕ	$[1.000 - 1.055]$	$34.80 \pm 0.92 \pm 0.64$	-	-
$\pi^+\pi^-\pi^0$ [above ϕ]	$[1.055 - 1.800]$	$2.45 \pm 0.26 \pm 0.03$	-	-
$\pi^+\pi^-2\pi^0$	$[1.020 - 1.800]$	$16.73 \pm 1.32 \pm 0.20$	$21.44 \pm 1.33 \pm 0.60$	-4.7 ± 1.8
$2\pi^+2\pi^-$	$[0.800 - 1.800]$	$13.95 \pm 0.90 \pm 0.23$	$12.34 \pm 0.96 \pm 0.40$	$+1.6 \pm 2.0$
$2\pi^+2\pi^-\pi^0$	$[1.019 - 1.800]$	$2.09 \pm 0.43 \pm 0.04$	-	-
$\pi^+\pi^-3\pi^0$ [2]	$[1.019 - 1.800]$	$1.29 \pm 0.22 \pm 0.02$	-	-
$3\pi^+3\pi^-$	$[1.350 - 1.800]$	$0.10 \pm 0.10 \pm 0.00$	-	-
$2\pi^+2\pi^-2\pi^0$	$[1.350 - 1.800]$	$1.41 \pm 0.30 \pm 0.03$	-	-
$\pi^+\pi^-4\pi^0$ [2]	$[1.350 - 1.800]$	$0.06 \pm 0.06 \pm 0.00$	-	-
$\eta(\to \pi^+\pi^-\gamma,\, 2\gamma)\pi^+\pi^-$	$[1.075 - 1.800]$	$0.54 \pm 0.07 \pm 0.01$	-	-
$\omega(\to \pi^0\gamma)\pi^0$	$[0.975 - 1.800]$	$0.63 \pm 0.10 \pm 0.01$	-	-
$\omega(\to \pi^0\gamma)(\pi\pi)^0$	$[1.340 - 1.800]$	$0.08 \pm 0.01 \pm 0.00$	-	-
K^+K^-	$[1.055 - 1.800]$	$4.63 \pm 0.40 \pm 0.06$	-	-
$K_S^0K_L^0$	$[1.097 - 1.800]$	$0.94 \pm 0.10 \pm 0.01$	-	-
$K^0K^\pm\pi^\mp$ [2]	$[1.340 - 1.800]$	$1.84 \pm 0.24 \pm 0.02$	-	-
$K\overline{K}\pi^0$ [2]	$[1.440 - 1.800]$	$0.60 \pm 0.20 \pm 0.01$	-	-
$K\overline{K}\pi\pi$ [2]	$[1.441 - 1.800]$	$2.22 \pm 1.02 \pm 0.03$	-	-
$R = \sum$ excl. modes	$[1.800 - 2.000]$	$8.20 \pm 0.66 \pm 0.10$	-	-
R [Data]	$[2.000 - 3.700]$	$26.70 \pm 1.70 \pm 0.00$	-	-
J/ψ	$[3.088 - 3.106]$	$5.94 \pm 0.35 \pm 0.03$	-	-
$\psi(2S)$	$[3.658 - 3.714]$	$1.50 \pm 0.14 \pm 0.00$	-	-
R [Data]	$[3.700 - 5.000]$	$7.22 \pm 0.28 \pm 0.00$	-	-
R_{udsc} [QCD]	$[5.000 - 9.300]$	$6.87 \pm 0.10 \pm 0.00$	-	-
R_{udscb} [QCD]	$[9.300 - 12.00]$	$1.21 \pm 0.05 \pm 0.00$	-	-
R_{udscbt} [QCD]	$[12.0 - \infty]$	$1.80 \pm 0.01 \pm 0.00$	-	-
$\sum (e^+e^- \to \text{hadrons})$	$[2m_{\pi^\pm} - \infty]$	$684.7 \pm 6.0_{\rm exp} \pm 3.6_{\rm rad}$	$709.0 \pm 5.1_{\rm exp} \pm 1.2_{\rm rad} \pm 2.8_{\rm SU(2)}$	$-24.3 \pm 7.9_{\rm tot}$

[1] Not including ω and ϕ resonances (see text).
[2] Using isospin relations (see text).
[3] e^+e^- data are used above 1.6 GeV (see text).

The contributions from the different processes in their indicated energy ranges are listed in Table 5. Wherever relevant, the two e^+e^-- and τ-based evaluations are given. The discrepancies discussed above are now expressed directly in terms of $a_\mu^{\rm had,LO}$ giving smaller estimates for e^+e^- data by

$$(-21.2 \pm 6.4_{\rm exp} \pm 2.4_{\rm rad} \pm 2.6_{\rm SU(2)}\,(\pm 7.3_{\rm total}))\ 10^{-10}$$

for the 2π channel and

$$(-3.1 \pm 2.6_{\rm exp} \pm 0.3_{\rm rad} \pm 1.0_{\rm SU(2)}\,(\pm 2.9_{\rm total}))\ 10^{-10}$$

for the sum of the 4π channels. The total discrepancy

$$(-24.3 \pm 6.9_{\rm exp} \pm 2.7_{\rm rad} \pm 2.8_{\rm SU(2)}\,(\pm 7.9_{\rm total}))\ 10^{-10}$$

amounts to 3.1 standard deviations and precludes from performing a straightforward combination of the two evaluations.

9.2 Results for a_μ

The results for the lowest order hadronic contribution are

$$a_\mu^{\rm had,LO} = (684.7 \pm 6.0_{\rm exp} \pm 3.6_{\rm rad})\ 10^{-10} \quad [e^+e^-\text{−based}]$$
$$a_\mu^{\rm had,LO} = (709.0 \pm 5.1_{\rm exp} \pm 1.2_{\rm rad} \pm 2.8_{\rm SU(2)})\ 10^{-10} \quad [\tau\text{−based}] \tag{30}$$

Adding the QED, higher-order hadronic, light-by-light scattering and weak contributions as given in Sect. 2, the results for a_μ are obtained

$$a_\mu^{\rm SM} = (11\,659\,169.3 \pm 7.0_{\rm had} \pm 3.5_{\rm LBL} \pm 0.4_{\rm QED+EW})\ 10^{-10} \quad [e^+e^-\text{−based}]\ ,$$
$$a_\mu^{\rm SM} = (11\,659\,193.6 \pm 5.9_{\rm had} \pm 3.5_{\rm LBL} \pm 0.4_{\rm QED+EW})\ 10^{-10} \quad [\tau\text{−based}]\ . \tag{31}$$

These values can be compared to the present experimental average given in (2). Adding experimental and theoretical errors in quadrature, the differences between measured and computed values are found to be:

$$a_\mu^{\rm exp} - a_\mu^{\rm SM} = (33.7 \pm 11.2)10^{-10} \quad [e^+e^-\text{−based}]\ ,$$
$$a_\mu^{\rm exp} - a_\mu^{\rm SM} = (9.4 \pm 10.5)10^{-10} \quad [\tau\text{−based}]\ , \tag{32}$$

corresponding to 3.0 and 0.9 standard deviations, respectively. A graphical comparison of the results (31) with the experimental value is given in Fig. 14. Also shown are our previous estimates [3,11] obtained before the CMD-2 and the new τ data were available (see discussion below), and the recent evaluation of Hagiwara et al. [129].

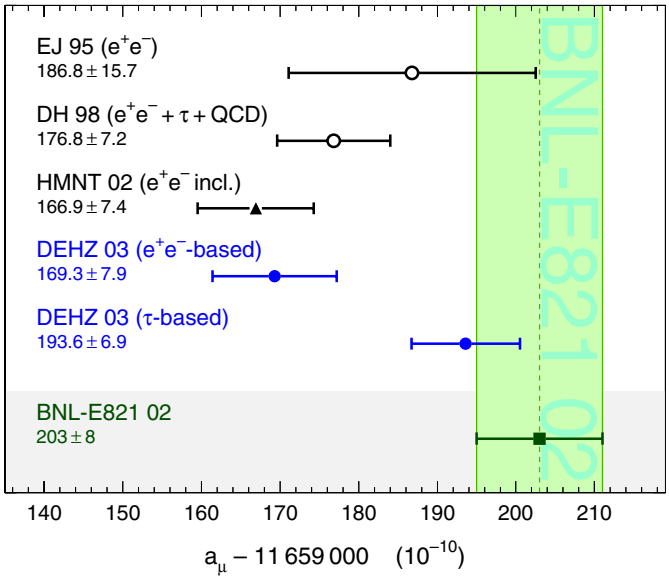

Fig. 14. Comparison of the results (31) with the BNL measurement [16]. Also shown are our previous estimates [3,11] obtained before the CMD-2 data were available, and the recent evaluation of Hagiwara et al. [129]

10 Discussion

10.1 The problem of the 2π contribution

The significant discrepancy between the e^+e^- and τ evaluations of $a_\mu^{\rm had,LO}$ is a matter of concern. In this section we comment on the relevant aspects of the problem. Since our earlier work [4,7,11] was based on a combined analysis of e^+e^- and τ data, we feel important to summarize the main changes (all expressed in 10^{-10} units) in the dominant 2π contribution where the τ contribution makes its impact:

- the new CMD-2 data [22] produce a downward shift of the e^+e^- evaluation by 1.9 (well within errors from previous experiments), while the final error is reduced from ±12.5 to ±5.1 with an additional ±2.4 from missing radiative corrections,
- the new ALEPH data [24] increases the τ evaluation by 3.5, which is within the previous experimental uncertainty of ±7.2 (in our previous analyses, we did not quote the results of a τ-based analysis alone, but only those from the combined spectral functions),
- including the CLEO data in the τ evaluation improves the precision, but further raises the central value by 4.0,
- although including the OPAL data has little effect on the overall precision, it also increases the result by 1.9,
- the new complete isospin symmetry-breaking correction, including the re-evaluation of the $S_{\rm EW}$ factor, increases the τ evaluation by 0.2 with respect to the previous one [4,7,11], which is well within the quoted error of ±2.5.

The previous (unpublished) difference between the e^+e^-- and τ-based evaluations of the 2π contributions,

$$\Delta\left(a_\mu^{\rm had,LO}\right)_{2\pi,ee-\tau} = -10.8 \pm 12.5_{\rm exp,ee} \pm 7.2_{\rm exp,\tau} \pm 2.5_{\rm SU(2)},$$

was consistent with zero, allowing the two spectral functions to be combined into an improved common estimate.

In spite of the fact that every change was within its previously estimated errors, the two results are not consistent anymore so that one must address the question of the possible origin of the problem. In principle, the observed discrepancy for the 2π contribution, (-21.2 ± 7.3), or $(-4.2 \pm 1.4)\%$ when expressed with respect to e^+e^-, could be caused by any (or the combination of several) of the following three effects which we examine in turn:

- **The normalization of e^+e^- data**
  Here, as below, 'normalization' does not necessarily mean an overall factor, but refers to the absolute scale of the 'bare' cross section at each energy point. There is no cross check of this at the precision of the new CMD-2 analysis. The only test we can provide is to compute the e^+e^- integral using the experiments separately. Because of the limited energy range where the major experiments overlap, we choose to perform the

integration in the range of $\sqrt{s}$ from 610.5 to 820 MeV. The corresponding contributions are: 313.5 ± 3.1 for CMD-2, 321.8 ± 13.9 for OLYA, 320.8 ± 12.6 for CMD, and 323.9 ± 2.1 for the isospin-corrected τ data. No errors on radiative corrections and isospin breaking are included in the above results.

– **The normalization of τ data**
The situation is quite similar, as the evaluation is dominated by the ALEPH data. It is also possible to compare the results provided by each experiment separately, with the spectral functions normalized to the respective hadronic branching ratios. Leaving aside the region below 500 MeV where a fit combining analyticity constraints is used, the contributions are: 460.1 ± 4.4 for ALEPH, 464.7 ± 9.3 for CLEO and 464.2 ± 8.1 for OPAL, where the common error on isospin breaking has been left out. The three values are consistent with each other and even the less precise values are not in good agreement with the e^+e^- estimate in this range, 440.8 ± 4.7, not including the error on missing radiative corrections. This is in line with the conclusion drawn from the comparison of branching ratios presented in Fig. 10. The larger values obtained with the CLEO and OPAL spectral functions are related to their relatively higher level below the ρ resonance, as can be observed in Fig. 3.
At the level of the $\tau \to \nu_\tau \pi^- \pi^0$ branching ratio, which controls the normalization of the $\pi^-\pi^0$ spectral function, stringent tests can be applied to the ALEPH results. We stress the fact that the branching fractions are obtained by a global procedure where all τ decay final states are considered, down to branching ratios of a few 10^{-4}, from a very clean initial sample [24]. The most critical part in the analysis is the separation of channels with different π^0 multiplicities. The $\pi^-\pi^0$ final state could be spoiled from the adjacent channels π^- and $\pi^-2\pi^0$ by inadequate understanding of the γ identification and the π^0 reconstruction. The observed branching ratios for these two modes are in agreement with expectations, based for the first one only on the assumption of universality of the $\mu - \tau$ couplings in the weak charged current (which is tested at the $3\ 10^{-3}$ level using the τ electronic branching ratio and the lifetime), and for the second one on the isospin relation with the $2\pi^-\pi^+$ branching ratio: $B_\pi - B_\pi^{\rm uni} = (-0.08 \pm 0.11_{\rm exp} \pm 0.04_{\rm th})\%$, and $B_{\pi 2\pi^0} - B_{\pi 2\pi^0}^{3\pi,{\rm iso}} = (+0.06 \pm 0.17_{\rm exp} \pm 0.07_{\rm th})\%$. These two tests provide confidence that the precise determination of the branching ratio for $\tau \to \nu_\tau \pi^- \pi^0$ is on solid ground, as the observed discrepancy would require a shift of 1.1% on this quantity. Apart from an overall normalization effect, differences could originate from the shape of the measured spectral functions. If all three spectral functions are normalized to the world average branching ratio (our final procedure), then the results for the contribution above 0.5 GeV become: 459.9 ± 3.6 for ALEPH, 465.4 ± 5.1 for CLEO and 464.5 ± 5.1 for OPAL, with a common error of ± 2.4 from the $\pi\pi^0$ and leptonic branching ratios and the uncertainty on isospin breaking left out. Again the results are consistent and their respective experimental errors give a better feeling of the relative impact of the measurements.

– **The isospin-breaking correction applied to τ data**
The basic components entering SU(2) breaking have been identified. The weak points before were the poor knowledge of the long-distance radiative corrections and the quantitative effect of loops. Both points have been addressed by the analysis of [30] showing that the effects are small and covered by the errors previously applied. The overall effect of the isospin-breaking corrections (including FSR) applied to the 2π τ data, expressed in relative terms, is $(-1.8 \pm 0.5)\%$. Its largest contribution (-2.3%) stems from the uncontroversial short-distance electroweak correction. Additional contributions must be identified to bridge the observed difference.
One could question the validity of the chiral model used. The authors of [30] argue that the corrections are insensitive to the details of their model and essentially depend only on the shape of the pion form factor. As the latter is known from experiment to adequate accuracy, there seems to be little space for improvement.

Thus we are unable at this point to identify the source of the discrepancy. More experimental and theoretical work is needed. On the experimental side, additional data is available from CMD-2, but not yet published. As an alternative, a promising approach using e^+e^- annihilation events with initial state radiation (ISR), as proposed in [133], allows a single experiment to cover simultaneously a broad energy range. Two experimental programs are underway at Frascati with KLOE [134] and at SLAC with BABAR [135]. The expected statistics are abundant, but it will be a challenge to reduce the systematic uncertainty at the level necessary to probe the CMD-2 results. However, the experimental technique being so different, it will be in any case valuable to compare the results with the present ones. As for τ's, the attention is now focused on the forthcoming results from the B factories. Again, the quality of the analysis will be determined by the capability to control systematics rather than the already sufficient statistical accuracy. On the theory side, the computation of more precise and more complete radiative corrections both for e^+e^- cross sections and τ decays should be actively pursued.

10.2 Other points of discussion

Other points are worth to be discussed: the 4π spectral functions, the ω and ϕ resonances and the sum of exclusive channels from 1.6 to 2 GeV.

As already pointed out in Sects. 6.1 and 6.2, the quality of both e^+e^- and τ data in the $2\pi^+2\pi^-$ and $\pi^+\pi^-2\pi^0$ final states is not as good as for the $\pi^+\pi^-$ channel. Agreement is observed in the former channel at the 10% level, while in the latter a large discrepancy is found (see the values in Table 5) which to this level cannot be attributed

to isospin breaking. Since significant differences are found within the e^+e^- data sets, we feel that it is a priority to clarify the experimental situation in this sector. The ISR program being conducted with the BABAR experiment should be able to shed some light upon this problem [135].

Compared to previous estimates, the ω and ϕ resonance contribution is now directly evaluated with the measured cross section, rather than integrating a Breit-Wigner function computed with averaged parameters. The ω value is basically unchanged, while a large downward shift of 4.3 has been found for the ϕ contribution. The origin of this change lies in the fact that the recent measurement of the ϕ lineshape yields a total width which is significantly smaller: Γ_ϕ decreased by 6σ in the last two years [105]!

Revisiting the situation of the exclusive channels in the 1.6-2 GeV range has led to significant changes, the origin of which are twofold: (*i*) more information (obtained in the study of τ decays, see Sect. 3.1) on the decay dynamics in the 6π channel could be used to bound the $\pi^+\pi^-4\pi^0$ contribution, and (*ii*) some data with poor quality were discarded, resulting in smaller contributions in the $3\pi^+3\pi^-$ and $2\pi^+2\pi^-2\pi^0$ channels. As a result, and unlike the conclusion reached in [136,129], we find the sum of the exclusive processes to be in reasonable agreement with the inclusive measurements of R in this range [86]. At any rate it is clear that better data should be taken in this energy region. The BABAR ISR physics program should be able to make an important contribution here as well.

Due to the last two points which are only relevant to e^+e^- data – the contribution from the ϕ resonance and the multi-pion channels – our new evaluation comes out to be significantly smaller than before.

10.3 Comparison to other evaluations of $a_\mu^{\rm had,LO}$

Here we restrict our discussion to recent evaluations which have been published since 1998, i.e. [137,138]. Previous estimates were considered in our earlier publication [11]. A common feature of [137,138] is that they use both e^+e^- and τ data for the 2π contribution. However, their analyses are based on the preliminary CMD-2 data [43] which are not corrected for vacuum polarization and FSR. Because of this, they fail to notice the discrepancy between e^+e^- and τ data. In addition, no mention of isospin symmetry breaking, and how to correct for it, is made in [137], shedding some doubts about the validity of the combination of the two data sets. The relatively high values obtained in these analyses compared to the present one are due in part to these problems.

The recent analysis of Hagiwara et al. [129] does include the final CMD-2 data. Our e^+e^--based result agrees with their evaluation using inclusive hadron production for energies above 1.6 GeV. However, as pointed out before, our re-evaluated sum of exclusive channels in this range is consistent within errors with the inclusive rate.

10.4 Consequences for $\alpha(M_Z^2)$

In spite of the fact that the present analysis was focused on the theoretical prediction for the muon magnetic anomaly, it is possible to draw some conclusions relevant to the evaluation of the hadronic vacuum polarization correction to the fine structure constant at M_Z^2. The problem found in the 2π spectral function is less important for $\Delta\alpha(M_Z^2)$ with respect to the total uncertainty, because the integral involved gives less weight to the low-energy region. The difference between the evaluations using the 2π, 4π and $2\pi2\pi^0$ spectral functions from e^+e^- and τ data are found to be:

$$\Delta\alpha^{ee}_{\rm had}(M_Z^2) \,-\, \Delta\alpha^{\tau}_{\rm had}(M_Z^2) = (-2.79 \pm \underbrace{0.43_{\rm ee} \pm 0.26_{\rm rad} \pm 0.55_{\tau} \pm 0.30_{\rm SU(2)}}_{0.80})10^{-4}.$$

While this low-energy contribution shows a 3.5 standard deviation discrepancy (when adding the different errors in quadrature), it also exceeds the total uncertainty of $1.6\ 10^{-4}$ on $\Delta\alpha(M_Z^2)$ which was quoted in [11]. It is worth pointing out that such a shift produces a noticeable effect for the determination of the Higgs boson mass $M_{\rm H}$ in the global electroweak fit [139]. With the present input for the electroweak observables [132] from LEP, SLC and FNAL yielding central values for $M_{\rm H}$ around 100 GeV, going from the e^+e^- to the τ-based evaluation induces a decrease of $M_{\rm H}$ by 16 GeV using all observables and by 20 GeV when only the most sensitive observable, $(\sin^2\theta_{\rm W})_{\rm eff}$, is used.

11 Conclusions

A new analysis of the lowest-order hadronic vacuum polarization contribution to the muon anomalous magnetic moment has been performed. It is based on the most recent high-precision experimental data from e^+e^- annihilation and τ decays in the $\pi\pi$ channel. Special attention was given to the problem of isospin symmetry breaking and the corresponding corrections to be applied to τ data. A new theoretical analysis of radiative corrections in τ decays was used and found to be in agreement with previous estimates. A complete re-evaluation of the contributions of e^+e^- annihilation cross sections in the energy range up to 2 GeV has been performed. Incorporating the recently corrected contribution from light-by-light scattering diagrams, the full prediction for the muon magnetic anomaly a_μ is obtained.

The main results of our analysis are the following:

- the new evaluation based solely on e^+e^- data is significantly lower than previous estimates and is in conflict with the experimental determination of a_μ by 3.0 standard deviations.
- the new precise evaluations of the dominant $\pi\pi$ contributions from e^+e^- annihilation and isospin-breaking corrected τ decays are not anymore in agreement with each other. A discussion has been presented for possible sources of the discrepancy which could not be

resolved. This situation is a matter of great concern, as the τ-based prediction of a_μ is in better agreement with the experimental value, from which it deviates by non-significant 0.9 standard deviations.

More experimental and theoretical work is needed to lift the present uncertainty on whether or not new physics has been uncovered with the muon magnetic moment.

Acknowledgements. It is a pleasure to thank our experimental colleagues from INP Novosibirsk, IHEP Beijing, LEP and Cornell for their essential contributions, and members of the Muon $(g-2)$ Collaboration for their keen interest. The close cooperation with V. Cirigliano, G. Ecker and H. Neufeld is warmly acknowledged. Informative discussions with F. Jegerlehner, J. H. Kühn, A. Pich, A. Stahl, A. Vainshtein and especially W. Marciano are appreciated. We thank S. Menke for providing us with the OPAL spectral functions.

References

1. N. Cabibbo, R. Gatto, Phys. Rev. Lett. **4**, 313 (1960); Phys. Rev. **124**, 1577 (1961); L.M. Brown, F. Calogero, Phys. Rev. **120**, 653 (1960)
2. C. Bouchiat, L. Michel, J. Phys. Radium **22**, 121 (1961)
3. S. Eidelman, F. Jegerlehner, Z. Phys. C **67**, 585 (1995)
4. R. Alemany, M. Davier, A. Höcker, Eur.Phys.J. C **2**, 123 (1998)
5. R. Barate et al., (ALEPH Collaboration), Z. Phys. C **76**, 15 (1997)
6. R. Barate et al., (ALEPH Collaboration), Eur. J. Phys. C **4**, 409 (1998)
7. M. Davier, A. Höcker, Phys. Lett. B **419**, 419 (1998)
8. J. H. Kühn, M. Steinhauser, Phys. Lett. B **437**, 425 (1998)
9. A.D. Martin, D. Zeppenfeld, Phys. Lett. B **345**, 558 (1995)
10. S. Groote et al., Phys. Lett. B **440**, 375 (1998)
11. M. Davier, A. Höcker, Phys. Lett. B **435**, 427 (1998)
12. J. Bailey et al., Phys. Lett. B **68**, 191 (1977). F.J.M. Farley, E. Picasso, "The muon $(g-2)$ Experiments", Advanced Series on Directions in High Energy Physics - Vol. 7 Quantum Electrodynamics, ed. T. Kinoshita, World Scientific 1990
13. R.M. Carey et al. (Muon $(g-2)$ Collaboration), Phys. Rev. Lett. **82**, 1632 (1999)
14. H.N. Brown et al. (Muon $(g-2)$ Collaboration), Phys. Rev. D **62**, 091101 (2000)
15. H.N. Brown et al. (Muon $(g-2)$ Collaboration), Phys. Rev. Lett. **86**, 2227 (2001)
16. G. W. Bennett et al. (Muon $(g-2)$ Collaboration), Phys. Rev. Lett. **89**, 101804 (2002); Erratum-ibid. **89**, 129903 (2002)
17. M. Hayakawa, T. Kinoshita, A.I. Sanda, Phys. Rev. D **54**, 3137 (1996); M. Hayakawa, T. Kinoshita, A.I. Sanda, Phys. Rev. Lett. **75**, 790 (1995)
18. J. Bijnens, E. Pallante, J. Prades, Nucl. Phys. B **474**, 379 (1996)
19. M. Knecht et al., Phys.Rev. D **65**, 073034 (2002)
20. M. Hayakawa, T. Kinoshita, Erratum Phys. Rev. D **66**, 019902 (2002); ibid. D **57**, 465 (1998)
21. J. Bijnens, E. Pallante, J. Prades, Nucl.Phys. B **626**, 410 (2002)
22. R.R. Akhmetshin et al. (CMD-2 Collaboration), Phys.Lett. B **527**, 161 (2002)
23. J.Z.Bai et al. (BES Collaboration), Phys. Rev. Lett. **84**, 594 (2000); Phys. Rev. Lett. **88**, 101802 (2002)
24. ALEPH Collaboration, ALEPH 2002-030 CONF 2002-019, (July 2002)
25. S. Anderson et al. (CLEO Collaboration), Phys.Rev. D **61**, 112002 (2000)
26. K. W. Edwards et al. (CLEO Collaboration), Phys.Rev. D **61**, 072003 (2000)
27. K. Ackerstaff et al. (OPAL Collaboration), Eur. Phys. J. C **7**, 571 (1999)
28. H. Czyż, J. H. Kühn, Eur.Phys.J. C **18**, 497 (2001)
29. V. Cirigliano, G. Ecker, H. Neufeld, Phys. Lett. B **513**, 361 (2001)
30. V. Cirigliano, G. Ecker, H. Neufeld, JHEP **0208**, 002 (2002)
31. T. Abe et al. (American Linear Collider Working Group), "Linear Collider Physics Resource Book for Snowmass 2001", SLAC-R-570, hep-ex/0106057 (2001)
32. V. W. Hughes, T. Kinoshita, Rev. Mod. Phys., **71**, S133 (1999)
33. A. Czarnecki, W.J. Marciano, Nucl. Phys. (Proc. Sup.) B **76**, 245 (1999)
34. B. Krause, Phys. Lett. B **390**, 392 (1997)
35. A. Czarnecki, W.J. Marciano, A. Vainshtein, hep-ph/0212229 (Dec. 2002); see also the earlier works: A. Czarnecki, B. Krause, W.J. Marciano, Phys. Rev. Lett. **76**, 3267 (1995); Phys. Rev. D **52**, 2619 (1995); R. Jackiw, S. Weinberg, Phys. Rev. D **5**, 2473 (1972); S. Peris, M. Perrottet, E. de Rafael, Phys. Lett. B **355**, 523 (1995); M. Knecht et al., JHEP **0211**, 003 (2002)
36. M. Gourdin, E. de Rafael, Nucl. Phys. B **10**, 667 (1969)
37. S.J. Brodsky, E. de Rafael, Phys. Rev. **168**, 1620 (1968)
38. L.M. Barkov et al. (OLYA, CMD Collaboration), Nucl. Phys. B **256**, 365 (1985)
39. I.B. Vasserman et al. (OLYA Collaboration), Sov. J. Nucl. Phys. **30**, 519 (1979)
40. I.B. Vasserman et al. (TOF Collaboration), Sov. J. Nucl. Phys. **33**, 368 (1981)
41. A. Quenzer et al. (DM1 Collaboration), Phys. Lett. B **76**, 512 (1978)
42. D. Bisello et al. (DM2 Collaboration), Phys. Lett. B **220**, 321 (1989)
43. R.R.Akhmetshin et al. (CMD-2 Collaboration), Preprint BudkerINP 1999-10, Novosibirsk (1999)
44. S.R. Amendolia et al. (NA7 Collaboration), Phys. Lett. B **138**, 454 (1984)
45. private communication from L. Rolandi, R. Tenchini
46. M. N. Achasov et al. (SND Collaboration), Phys. Rev. D **63**, 072002 (2001)
47. R. R. Akhmetshin et al. (CMD-2 Collaboration), Phys. Lett. B **476**, 33 (2000)
48. R. R. Akhmetshin et al. (CMD-2 Collaboration), Phys. Lett. B **466**, 385 (1999), Erratum-ibid. B **508**, 217 (2001)
49. M.N.Achasov et al. (SND Collaboration), Preprint BudkerINP 2001-54, Novosibirsk (2001)
50. R.R.Akhmetshin et al. (CMD-2 Collaboration), Phys. Lett. B **509**, 217 (2001)
51. S.J. Dolinsky et al. (ND Collaboration), Phys. Rep. C **202**, 99 (1991)

52. A. Cordier et al. (DM1 Collaboration), Nucl. Phys. B **172**, 13 (1980)
53. A. Antonelli et al. (DM2 Collaboration), Z. Phys. C **56**, 15 (1992)
54. M.N. Achasov et al. (SND Collaboration), Phys. Rev. D **66**, 032001 (2002)
55. L. M. Barkov et al. (CMD Collaboration), Preprint INP 89-15, Novosibirsk (1989)
56. G. Cosme et al. (M3N Collaboration), Nucl. Phys. B **152**, 215 (1979); C. Paulot, Thesis, LAL-79-14, Orsay (1979)
57. L.M. Kurdadze et al. (OLYA Collaboration), JETP Lett. **43**, 643 (1986)
58. D. Bisello (for the DM2 Collaboration), Nucl. Phys. B **21** (Proc. Suppl.) (1991) 111
59. D. Bisello et al. (DM2 Collaboration), Report LAL-90-35, Orsay (1990)
60. L. Stanco (for the DM2 Collaboration), Proceedings of Hadron-91, World Scientific ed. 84 (1992)
61. R.R.Akhmetshin et al. (CMD-2 Collaboration), Phys. Lett. B **466**, 392 (1999)
62. M.N.Achasov et al. (SND Collaboration), Preprint BudkerINP 2001-34, Novosibirsk (2001)
63. M.N.Achasov et al. (SND Collaboration), Phys. Lett. B **486**, 29 (2000)
64. L.M. Kurdadze et al. (OLYA Collaboration), JETP Lett. **47**, 512 (1988)
65. L.M. Barkov et al. (CMD Collaboration), Sov. J. Nucl. Phys. **47**, 248 (1988)
66. A. Cordier et al. (DM1 Collaboration), Phys. Lett. B **109**, 129 (1982)
67. A. Cordier et al. (DM1 Collaboration), Phys. Lett. B **81**, 389 (1979)
68. A.Cordier et al. (DM1 Collaboration), Phys. Lett. **106**B, 155 (1981)
69. R.R.Akhmetshin et al. (CMD-2 Collaboration), Phys. Lett. B **489**, 125 (2000)
70. D. Bisello et al. (DM1 Collaboration), Phys. Lett. B **107**, 145 (1981)
71. M. Schioppa (DM2 Collaboration), Thesis, Universita di Roma "La Sapienza" (1986)
72. A. Anastassov et al. (CLEO Collaboration), Phys. Rev. Lett. **86**, 4467 (2001)
73. T. Bergfeld et al. (CLEO Collaboration), Phys. Rev. Lett. **79**, 2406 (1997); A. Weinstein, Proceedings of the $6^{\rm th}$ International Workshop on τ Lepton Physics, Victoria 2000, R. J. Sobie, J. M. Roney eds., North Holland (2001)
74. P.M. Ivanov et al. (OLYA Collaboration), Phys. Lett. B **107**, 297 (1981); P.M. Ivanov et al. (OLYA Collaboration), JETP. Lett. **36**, 112 (1982)
75. B.Delcourt et al. (DM1 Collaboration), Phys. Lett. **99**B (1981) 257; F.Mané et al. (DM1 Collaboration), Phys. Lett. **99B**, 261 (1981)
76. D. Bisello et al. (DM2 Collaboration), Z. Phys. C **39**, 13 (1988)
77. G. V. Anikin et al. (CMD Collaboration), Preprint INP 83-35, Novosibirsk (1983)
78. R.R.Akhmetshin et al. (CMD-2 Collaboration), Phys. Lett. B **551**, 27 (2003)
79. A. Cordier et al. (DM1 Collaboration), Phys. Lett. B **110**, 335 (1982)
80. F. Mané et al. (DM1 Collaboration), Phys. Lett. B **112**, 178 (1982)
81. F. Mané (DM1 Collaboration), Thesis, Université de Paris-Sud, LAL 82/46 (1982)
82. D.Bisello et al. (DM2 Collaboration), Z. Phys. C **52**, 227 (1991)
83. B.Delcourt et al. (DM1 Collaboration), Phys. Lett. **86**B, 395 (1979)
84. D.Bisello et al. (DM2 Collaboration), Nucl. Phys. B **224**, 379 (1983)
85. A.Antonelli et al. (FENICE Collaboration), Nucl. Phys. B **517**, 3 (1998)
86. C. Bacci et al. ($\gamma\gamma$2 Collaboration), Phys. Lett. B **86**, 234 (1979)
87. J.L. Siegrist et al. (MARK I Collaboration), Phys. Rev. D **26**, 969 (1982)
88. W. Bacino et al. (DELCO Collaboration), Phys. Rev. Lett. **40**, 671 (1978)
89. R. Brandelik et al. (DASP Collaboration), Phys. Lett. B **76**, 361 (1978); H. Albrecht et al. (DASP Collaboration), Phys. Lett. B **116**, 383 (1982)
90. J. Burmester et al. (PLUTO Collaboration), Phys. Lett. B **66**, 395 (1977); C. Berger et al. (PLUTO Collaboration), Phys. Lett. B **81**, 410 (1979); L. Criegee, G. Knies (PLUTO Collaboration), Phys. Rep. C **83**, 151 (1982)
91. B. Niczyporuk et al. (LENA Collaboration), Z. Phys. C **15**, 299 (1982)
92. Z. Jakubowski et al. (Crystal Ball Collaboration), Z. Phys. C **40**, 49 (1988); C. Edwards et al. (Crystal Ball Collaboration), SLAC-PUB-5160 (1990)
93. A. Osterheld et al. (Crystal Ball Collaboration), SLAC-PUB-4160 (1986)
94. A.E. Blinov et al. (MD-1 Collaboration), Z. Phys. C **49**, 239 (1991); A.E. Blinov et al. (MD-1 Collaboration), Z. Phys. C **70**, 31 (1996)
95. H.J. Behrend et al. (CELLO Collaboration), Phys. Lett. B **183**, 400 (1987)
96. W. Bartel et al. (JADE Collaboration), Phys. Lett. B **129**, 145 (1983); W. Bartel et al. (JADE Collaboration), Phys. Lett. B **160**, 337 (1985); B. Naroska (JADE Collaboration), Phys. Rep. C **148**, 67 (1987)
97. B. Adeva et al. (MARK-J Collaboration), Phys. Rev. Lett. **50**, 799 (1983); B. Adeva et al. (MARK-J Collaboration), Phys. Rev. Lett. **50**, 2051 (1983); B. Adeva et al. (MARK-J Collaboration), Phys. Rep. C **109**, 131 (1984); B. Adeva et al. (MARK-J Collaboration), Phys. Rev. D **34**, 681 (1986)
98. R. Brandelik et al. (TASSO Collaboration), Phys. Lett. B **113**, 499 (1982); M. Althoff et al. (TASSO Collaboration), Phys. Lett. B **138**, 441 (1984)
99. R. Giles et al. (CLEO Collaboration), Phys. Rev. D **29**, 1285 (1984); D. Besson et al. (CLEO Collaboration), Phys. Rev. Lett. **54**, 381 (1985); P.Ammar et al. (CLEO Collaboration), Phys. Rev. D **57**, 1350 (1998)
100. E. Rice et al. (CUSB Collaboration), Phys. Rev. Lett. **48**, 906 (1982)
101. E. Fernandez et al. (MAC Collaboration), Phys. Rev. D **31**, 1537 (1985)
102. H. Burkhardt, F. Jegerlehner, G. Penso, C. Verzegnassi, Z. Phys. C **42**, 497 (1989)
103. D. Buskulic et al. (ALEPH Collaboration), Z. Phys. C **70**, 579 (1996)
104. P. Tsai, Phys. Rev. D **4**, 2821 (1971)
105. Review of Particle Physics, K.Hagiwara et al., Phys. Rev. D **66**, 010001 (2002)

106. S. Jadach, J. H. Kühn, Z. Wąs, Comp. Phys. Comm., **64**, 275 (1991)
107. E. Barberio, Z. Wąs, Comp. Phys. Comm., **79**, 291 (1994)
108. G. Bonneau, F. Martin, Nucl. Phys. B **27**, 381 (1971)
109. S. Eidelman, E. Kuraev, Phys. Lett. B **80**, 94 (1978)
110. M. L. Swartz, Phys. Rev. D **53**, 5268 (1996)
111. A. Höfer, J. Gluza, F. Jegerlehner, Eur. Phys. J. C **24**, 51 (2002)
112. W. Marciano, A. Sirlin, Phys. Rev. Lett. **61**, 1815 (1988)
113. E. Braaten, S. Narison, A. Pich, Nucl. Phys. B **373**, 581 (1992)
114. We thank V. Cirigliano, A. Pich for pointing out this fact to us, W. Marciano for further clarification on this point. See also the discussion in: J. Erler, hep-ph/0211345 (2002)
115. W. Marciano, A. Sirlin, Phys. Rev. Lett. **56**, 22 (1986)
116. A. Sirlin, Nucl. Phys. B **196**, 83 (1982)
117. E. Braaten, C.S. Li, Phys. Rev. D **42**, 3888 (1990)
118. R. Decker, M. Finkemeier, Nucl. Phys. B **438**, 17 (1995)
119. J. Bijnens, P. Gosdzinsky, Phys. Lett. B **388**, 203 (1996)
120. M. N. Achasov et al. (SND Collaboration), Phys. Rev. D **65**, 032002 (2002)
121. P. Singer, Phys. Rev. **130**, 2441 (1963); Erratum-ibid. **161**, 1694 (1967)
122. S. Tisserant, T.N. Truong, Phys. Lett. B **115**, 264 (1982); A. Pich, Phys. Lett. B **196**, 561 (1987); H. Neufeld, H. Rupertsberger, Z. Phys. C **68**, 91 (1995)
123. F. Guerrero, A. Pich, Phys. Lett. B **412**, 382 (1997); D. Gómez Dumm, A. Pich, J. Portolés, Phys. Rev. D **62**, 054014 (2000)
124. M. Artuso et al. (CLEO Collaboration), Phys. Rev. Lett. **72**, 3762 (1994)
125. K. Ackerstaff et al. (OPAL Collaboration), Eur. Phys. J. C **4**, 93 (1998)
126. R. Barate et al. (ALEPH Collaboration), Eur. Phys. J. C **11**, 599 (1999)
127. M. Battle et al. (CLEO Collaboration), Phys. Rev. Lett. **73**, 1079 (1994)
128. S.R. Amendolia et al. (NA7 Collaboration), Nucl. Phys. B **277**, 168 (1986)
129. K. Hagiwara, A.D. Martin, D. Nomura, T. Teubner, KEK-TH-844, IPPP-02-52, DCPT-02-104, CERN-TH-2002-233, hep-ph/0209187 (2002); T. Teubner, Talk given at ICHEP'02, Amsterdam, The Netherlands, 2002
130. L.R. Surguladze, M.A. Samuel, Phys. Rev. Lett. **66**, 560 (1991); S.G. Gorishny, A.L. Kataev, S.A. Larin, Phys. Lett. B **259**, 144 (1991)
131. K.G. Chetyrkin, J.H. Kühn, M. Steinhauser, Nucl. Phys. B **482**, 213 (1996)
132. LEP Electroweak Working Group, LEPEWWG/2002-01 (May 2002)
133. S. Binner, J.H. Kühn, K. Melnikov, Phys. Lett. B **459**, 279 (1999)
134. G. Cataldi et al. (KLOE Collaboration), in Physics, Detectors for DAPHNE (1999) 569
135. E. P. Solodov (BABAR Collaboration), hep-ex/0107027 (2001)
136. A.D. Martin, J. Outhwaite, M.G. Ryskin, Phys. Lett. B **492**, 69 (2000)
137. S. Narison, Phys. Lett. B **513**, 53 (2001), Erratum-ibid. **526**, 414 (2002)
138. J. F. Trocóniz, F. Ynduráin, Phys. Rev. D **65**, 093001 (2002)
139. K. Hagiwara, S. Matsumoto, D. Haidt, C.S. Kim, Z. Phys. C **64**, 559 (1994)